Structural Evolution of Thakkhola Graben: Implications for the Architecture of the Central Himalaya, Nepal

---

A Thesis

Presented to

the Faculty of the Department of Earth and Atmospheric Sciences

University of Houston

In Partial Fulfillment

of the Requirements for the Degree

Master of Science

By

Thomas Baltz

December 2012

Structural Evolution of Thakkhola Graben: Implications for the Architecture of the Central Himalaya, Nepal

Thomas Baltz

APPROVED:

Dr. Michael Murphy, Committee Chair

Dr. Peter Copeland, Committee

Dr. Michael H. Taylor, Committee

Dr. Mark A. Smith

Dean, College of Natural Sciences and Mathematics

Acknowledgements

I would like to Dr. Michael Murphy for being a supportive mentor throughout my research. He is the epitome of a field geologist. I find him a constant source of inspiration and enthusiasm. I would also like to thank Dr. Peter Copeland and Dr. Michael Taylor for being a part of my research committee. Their constructive criticism and insight has contributed to the development of this thesis and my philosophy as a scientist. I would like to thank Dr. Jack Casey, Dr. Alex Robinson, and Dr. Veronica Sanchez for inspiring me to become a graduate student in structural geology and tectonics. Without them I might have become just a geophysicist. I would like to thank Mr. Bhim Chand of Earth Paradise Expeditions for providing such excellent logistical and cultural support in the Nepal Himalaya. Finally, I would like to thank Mr. Adrian Gittens and Mr. Calvin Silver for many fruitful discussions while hiking around in the mountains.

Structural Evolution of Thakkhola Graben: Implications for the Architecture of the Central Himalaya, Nepal

A Thesis

Presented to

the Faculty of the Department of Earth and Atmospheric Sciences

University of Houston

In Partial Fulfillment

of the Requirements for the Degree

Master of Science

By

Thomas Baltz

December 2012

Abstract

The Thakkhola Graben of central Nepal is one of several north-south-trending rifts and grabens throughout the Himalayan hinterland and southern Tibet. The faults bounding the graben run from the crest of the Himalayas at the Annapurna and Dhaulagiri Ranges to the suture between India and Asia. This suture is reported to separate two disparate stress regimes, arc-perpendicular compression in the Nepal Himalayas to the south and arc-parallel extension in the Tibetan Plateau to the north. However, two lines of evidence suggest the India-Asia Suture no longer functions as a structural boundary between these stress fields: (1) the Lopukangri Rift cuts and offsets the suture, and (2) the Thakkhola Graben is located south of the suture. Despite decades of research in the Thakkhola Graben, an accurate account of fault geometry and kinematics has yet to be presented. Therefore its relationship to extensional structures in Tibet and its role in Himalayan tectonics is undetermined. Field mapping, combined with kinematic modeling and reconstruction of offset piercing points, has confined the geometry and kinematics of the faults bounding the Thakkhola Graben. The western boundary of the graben is the Dangardzang Fault and the eastern boundary is the Muktinath Fault, both of which are steeply dipping and cut down into the middle crust. The Dangardzang Fault consists of two parallel fault strands, with the easternmost accommodating the majority of strain. This fault has accommodated 4.5 kilometers of dip-slip displacement, 5.3 kilometers of dextral strike-slip displacement, and 1.4 kilometers of horizontal extension. The Muktinath Fault consists of one dominant fault strand with several subsidiary faults of lesser magnitude. This fault has accommodated

4.2 kilometers of dip-slip displacement, 1.9 kilometers of sinistral strike-slip displacement, and 0.8 kilometers of horizontal extension. Comparison of the Thakkhola Graben with the Lopukangri Rift to the north shows both of these structures share similar fault geometries, magnitudes of slip, and kinematics. This relationship implies the same stress field is active on both sides of the India-Asia Suture and therefore, in this region it no longer operates as a structural boundary between the Himalayas and Tibet.

Contents

Introduction

GPS measurements suggest the Himalayas and southern Tibet are extending in an approximately E-W direction. Jade et al. (2004) determine a change of 17.8 ± 1 mm/yr in arc length of a great circle connecting Leh (78^{o}E) to Lhasa (91^{o}E) in an approximately east-west direction. Using an India-fixed reference frame, Chen et al. (2004) shows extension of 26 ± 3 mm/yr directed N110^{o}E from Shiquanhe (80^{o}E) to Gangbu (93^{o}E). This work also shows extension of 13 ± 2 mm/yr directed N110^{o}E from Simikot (82^{o}E) to Lhasa (91^{o}E). These data suggest a non-uniform amount of extensional strain in a direction parallel to the arc of the Himalayas.

Within the northernmost Himalayas and southern Tibet a number of extensional features have been observed to accommodate arc-parallel extension. These include, but are not limited to, the Karakoram Fault (e.g. Armijo et al., 1989; Murphy et al., 2000), the Leo Pargil dome (Thiede et al., 2006), the Gurla Mandhata dome (Murphy et al., 2002), the Humla Fault (Murphy and Copeland, 2005), the Tibrikot Fault (Nakata et al., 1990; Styron et al., 2009), the Thakkhola Graben (e.g. Colchen, 1999; Hurtado et al., 2001; Baltz and Murphy, 2009), the Lopukangri Rift (Murphy et al., 2010), the Kung Co Rift (Lee et al., 2011), and the Ama Drime massif (Jessup et al., 2008; Kali et al., 2010) (fig. 1). There is a variation in the magnitude of arc-parallel extension these structures have accommodated; ranging from 100's of kilometers in the case of the Karakoram Fault to 10's of kilometers for normal faults within Nepal (Styron et al., 2011).

The Thakkhola Graben (fig. 1) is the only north-south-oriented normal fault in Nepal to cut through the high peaks of the Himalayas and is the most geomorphologically prominent of these structures (Colchen, 1999). It has been used in a variety of models

Figure 1

Tectonostratigraphic map of Himalayas and southern Tibet with the country of Nepal outlined in white. Lithotectonic units include Lhasa terrane in southern Tibet, Tethyan Sedimentary sequence within the Himalayan hinterland of southern Tibet and northern Nepal, Greater Himalayan crystallines within the crest of the Himalayas of Nepal, Lesser Himalayan sequence south of the crest of the Himalayas in Nepal, and the Siwalik rocks within the Himalayan foreland of southern Nepal and northern India. BNS - Bangong-Nujiang Suture, IYS - Indus - Yalu Suture, STD - South Tibetan Detachment, MCT- Main Central Thrust, MBT - Main Boundary Thrust, MFT - Main Frontal Thrust, KF - Karakoram Fault, LK - Lopukangri Rift, TY - Tangra Yum-Co Rift, LP - Leo Pargil Detachment, GM - Gurla Mandhata Detachment, HF - Humla Fault, TF - Tibrikot Fault, TG - Thakkhola Graben, KC - Kung Co Rift, AD - Ama Drime Rift. Modified from Robinson, D. et al., 2001; Taylor and Yin, 2009; Styron et al., 2011.

Figure 1

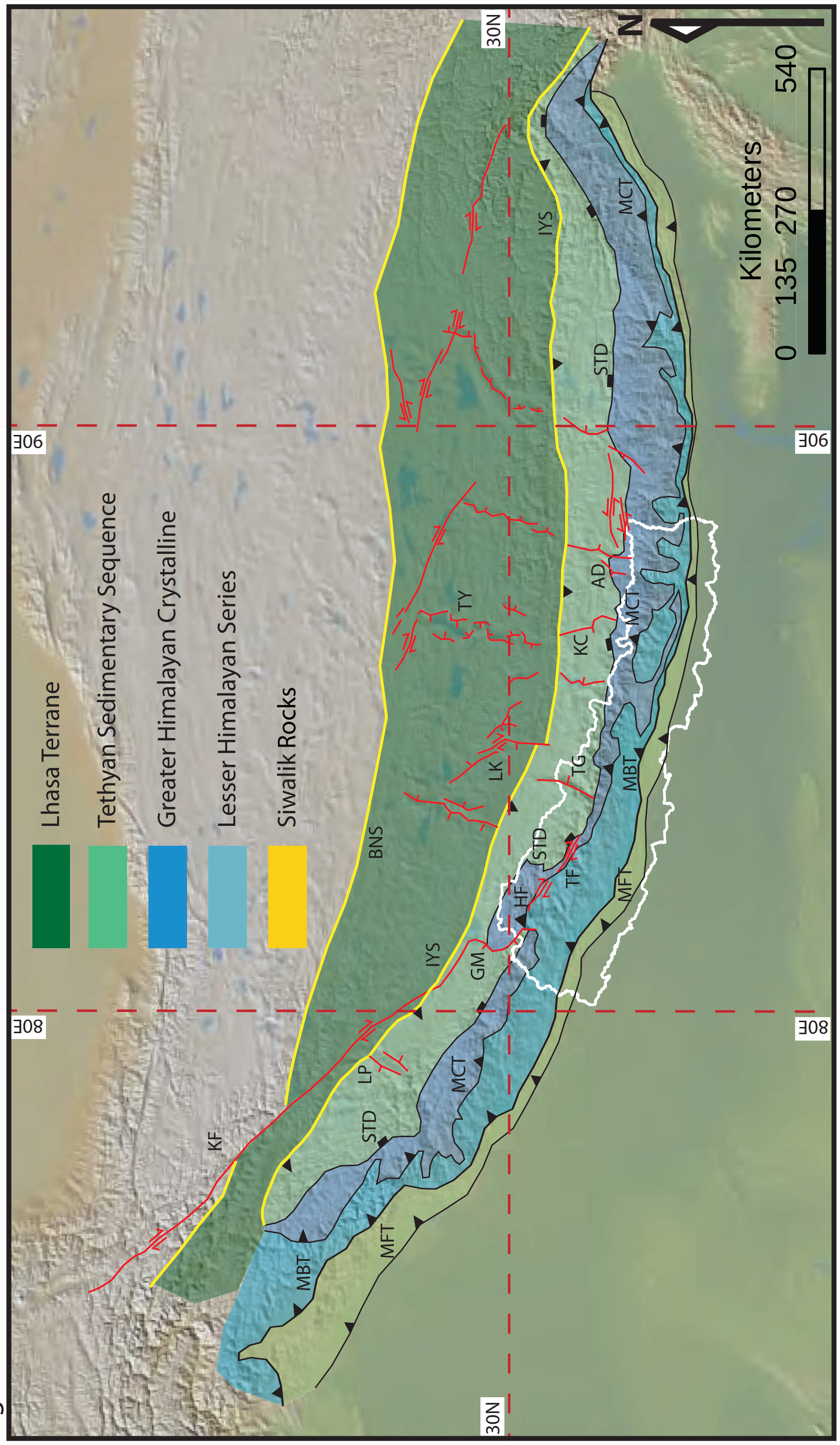

Lhasa Terrane
Tethyan Sedimentary Sequence
Greater Himalayan Crystalline
Lesser Himalayan Series
Siwalik Rocks
Kilometers
0 135 270 540
N
30N
90E
80E
KF
BNS
IYS
LP
STD
MCT
MBT
MFT
GM
HF
TF
TG
LK
TY
KC
AD

which attempt to describe the kinematics of the Himalayas and southern Tibet; e.g. lateral extrusion (Tapponnier et al., 1982; Peltzer and Tapponnier, 1988), oroclinal bending (Klootwijk et al., 1985; Ratschbacher et al., 1994; Schill et al., 2004), radial spreading (Jade et al., 2004; Murphy and Copeland, 2005; Copley and McKenzie, 2007), and oblique convergence (McCaffrey and Nabelek, 1998; Seeber and Pecher, 1998). Despite decades of research (e.g. Hagen, 1959; Bassoullet and Colchen, 1974; Molnar and Tapponnier, 1978; Colchen et al., 1980; Fort et al., 1982; Colchen, 1999; Hurtado et al., 2001; Godin, 2003) the magnitude of slip accommodated by the Thakkhola Graben is still not certain. Predictions based on modeling and plate reconstructions estimate as much as 45 kilometers of slip may have been accommodated here (Replumaz and Tapponier, 2003); other authors predict as little as 3 kilometers (Colchen, 1999). Determining the magnitude of slip and arc-parallel extension accommodated by the Thakkhola Graben is essential to the development of orogen-scale kinematic models.

This paper will provide a field-based structural study of the Thakkhola Graben combined with geometrical and kinematic analysis to determine its role in the tectonic evolution of the Himalayas. Geologic mapping has constrained the distribution and orientation of the various mappable units as well as the geometry of faults. The net magnitude and direction of slip accommodated by the basin-bounding faults has been determined by geometrical restoration of offset piercing points along both faults. This information is used to evaluate the Thakkhola Graben’s role in accommodating arc-parallel strain.

Geologic Background

Deformation within the Himalayas and southern Tibet can be categorized into two sets; features accommodating arc-perpendicular strain and features accommodating arc-parallel strain. These two sets are distinct with respect to their position within the arc as well as their timing within the history of the orogen. Arc-perpendicular compression within the Himalayas has been accommodated through a foreland propagating thrust system that roots into a common decollement known as the Main Himalayan Thrust (Zhao et al., 1993). This system consists of, from oldest to youngest, the Main Central Thrust, the Main Boundary Thrust, and the Main Frontal Thrust. The Main Central Thrust (fig. 1), found south of the Himalayan crest, was active from 22-15 Ma with possible reactivation at 8 Ma (Hodges et al., 1996; Harrison et al., 1997). The Main Boundary Thrust (fig. 1) to the south was active from ~11 Ma through the Pleistocene (Burbank et al., 1996). The Main Frontal Thrust (fig. 1) is the southernmost of these thrusts and currently accommodates convergence between India and the Himalayas. This fault was activated during the Pliocene and has been observed to cut quaternary sediments (Molnar et al., 1984; Yin and Harrison, 2000). Arc-perpendicular extension has been accommodated by the South Tibetan Detachment System. The South Tibetan Detachment System (fig. 1) has been mapped all along the trend of the orogen and it is found north of the Main Central Thrust within the highest topography of the Himalayas (Burchfiel, 1985; Wu et al., 1998; Murphy and Harrison, 1999; Searle and Godin, 2003; Leloup et al., 2010). Initiation of slip on the South Tibetan Detachment System is understood to have been active in the middle and possibly early Miocene (Noble and Searle, 1995; Edwards and Harrison, 1997; Wu et al., 1998; Murphy and Harrison, 1999). Cessation of motion along the South Tibetan Detachment System occurred at around 8-14 Ma through the development of north-south-trending rifts and grabens which cut and offset the detachment (Burchfiel et al., 1992; Harrison et al., 1995; Wu et al., 1998). This cross-cutting relationship is observed throughout the Himalayas.

Geologic Setting

The Thakkhola Graben is located in the Kali Gandaki Valley of central Nepal, north of the Annapurna Detachment of the South Tibetan Detachment System (fig. 2). The Annapurna Detachment has been mapped high in the Annapurna and Dhaulagiri Ranges as a 1500 meter thick brittle-ductile shear zone between unmetamorphosed Tethyan Sedimentary sequence rocks in the hanging wall and Greater Himalayan crystalline rocks in the footwall (Brown and Nazarchuk, 1993; Godin et al., 1999a; Godin, 2003). The base of the Annapurna shear zone in the Kali Gandaki Valley has been correlated with the Deorali Detachment (Hodges et al., 1996) in the Modi Khola region and the Chame Detachment in the Manaslu region (Searle and Godin, 2003). This is a zone of high shear entirely within the Greater Himalayan metamorphic rocks operating at 22.5-18 Ma (Hodges et al., 1996, Godin et al., 2001). The top of the Annapurna shear zone has been correlated with the Machhapuchhare Detachment in the Modi Khola region (Hodges et al., 1996) and the Phu Detachment in the Manaslu region (Searle and Godin, 2003) (fig. 2). This upper boundary separates unmetamorphosed Tethyan Sedimentary sequence rocks from metamorphosed Tethyan and Greater Himalayan crystalline rocks. The Phu Detachment to the east marks the boundary between the Tethyan rocks and the Manaslu Leucogranite, no leucogranite veins or dykes are found in the hanging wall. As such, the upper boundary of the Annapurna shear zone corresponds with the true South

Figure 2

Regional geologic map of central Nepal and southern Tibet modified from Geological Map of Nepal (1:1,000,000 scale), 2002; Searle and Godin, 2003. The bounding faults of the Thakkhola Graben cut and offset previously folded and faulted Tethyan Sedimentary sequence and granitic rocks. Depicts the South Tibetan Detachment composed of an upper brittle detachment and a lower ductile shear zone (Hodges et al., 1996; Godin et al., 1999b; Searle and Godin, 2003) Major cities are marked with black and white circles, major peaks are marked with black and white triangles. DF - Dangardzang Fault, MF - Muktinath Fault, STD - South Tibetan Detachment, MCT I - Main Central Thrust (upper), MCT II - Main Central Thrust (lower), PZ - Paleozoic age rocks, MZ - Mesozoic age rocks, N - Neogene age rocks, TSS - Tethyan Sedimentary sequence, MTSS - Metamorphosed Tethyan Sedimentary sequence, GHC- Greater Himalayan crystallines, LHS - Lesser Himalayan series.

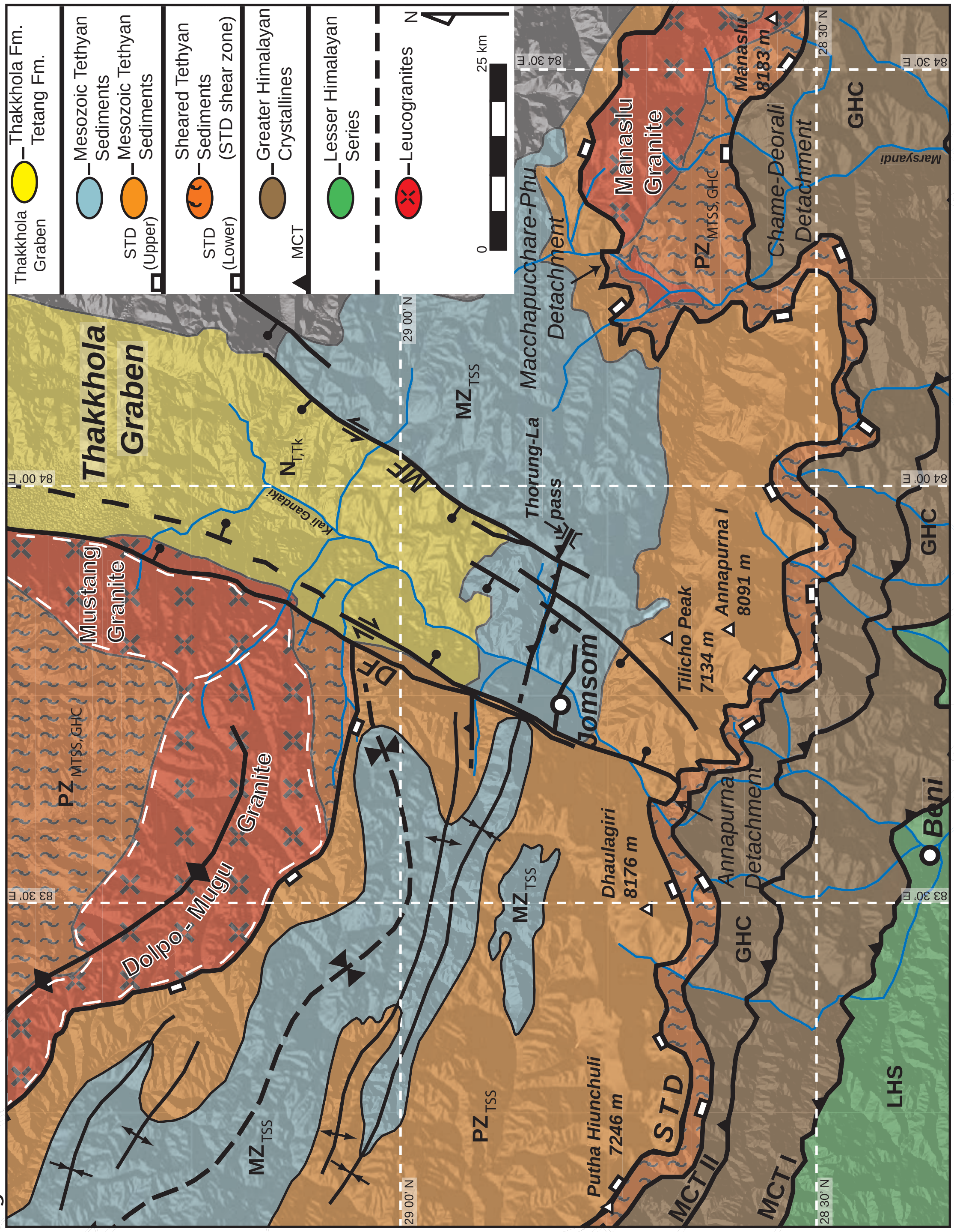

Thakkhola Graben
Thakkhola Fm.
Tetang Fm.
Mesozoic Tethyan Sediments
STD (Upper)
Mesozoic Tethyan Sediments
STD (Lower)
Sheared Tethyan Sediments (STD shear zone)
Greater Himalayan Crystallines
MCT
Lesser Himalayan Series
Leucogranites
N
0
25 km
Thakkhola Graben
Mustang Granite
Dolpo - Mugu Granite
Manaslu Granite
Macchapucchare-Phu Detachment
Thorung-La pass
Jomsom
Tilicho Peak 7134 m
Annapurna I 8091 m
Dhaulagiri 8176 m
Putha Hiunchuli 7246 m
Manaslu 8183 m
Annapurna Detachment
Chame-Deorali Detachment
Kali Gandaki
Marsyandi
Beni
STD
MCT II
MCT I
GHC
LHS
DF
MF
29 00' N
28 30' N
83 30' E
84 00' E
84 30' E

Figure 2

Tibetan det Detachment achment and was active at 19 – 14 Ma (Hodges et al., 1996; Searle and Godin, 2003). The bounding faults of the Thakkhola Graben have been previously mapped to cut and offset folded Tethyan sedimentary sequence rocks as well as the Mustang Leucogranite (Bordet et al., 1971; Colchen, 1999; Godin, 2003). Recent work shows the graben-bounding faults cut through the Annapurna shear zone into the underlying Greater Himalayan rocks (Baltz and Murphy, 2009) (fig. 2). Operation of the Thakkhola Graben faults began definitively by 11 Ma based on the youngest age for basin-fill sediment (Garzione et al., 2000) and even as early as 14 Ma based upon the age of a N-S oriented extensional vein in the adjacent Marsyandi Valley (Coleman and Hodges, 1995).

Greater Himalayan Crystallines (GHC)

The Greater Himalayan crystalline rocks make up the footwall of the Annapurna Detachment (Brown and Nazurchuck, 1993; Godin et al., 1999a). These have been divided into three mappable formations by Le Fort (1975), Formation I, Formation II, and Formation III. In the Kali Gandaki region Formation I consists of kyanite-garnet-two-mica banded gneiss. The overlying Formation II is marked by a thick quartzite bed followed by alternating pyroxene and amphibole bearing calc-silicate gneisses and marbles. Formation III is composed of pelitic gneisses capped by granitic augen gneiss. In the Kali Gandaki region, exposure of GHC rocks is restricted to the front of the Annapurna and Dhaulagiri Ranges as well as in the northern portion of the western footwall of the Thakkhola Graben (fig. 2). In our mapping area the GHC was infrequently encountered and only exposed in remote areas, as such we have mapped the GHC as undifferentiated. The portions of the GHC mapped in the graben footwall consisted of garnet-biotite gneisses, calc silicate gneisses, and marbles. The GHC in the graben footwall is observed to be highly penetrated by leucogranite dikes and sills.

Dolpo-Mugu and Mustang Leucogranites

Two leucogranite bodies are exposed in the NW portion of the western graben-bounding footwall; the Dolpo-Mugu Leucogranite and the Mustang Leucogranite (fig. 2). The Dolpo-Mugu Leucogranite is the larger of these two, stretching at least 300-400 kilometers to the west; while the Mustang Leucogranite is located just around the western boundary fault of the Thakkhola Graben. Both of these granites are interpreted to belong to the younger of two Himalayan granite belts, the North Himalayan Granite Belt (Debon et al., 1986; Harrison et al., 1999). Harrison et al. (1999) dated one monazite sample from the Dolpo-Mugu Leucogranite and determined an age of 17.6 Ma, this was evaluated as more consistent with North Himalayan Granite Belt ages, 15-9 Ma (Scharer et al., 1986; Zhang et al., 2004), rather than with the older High Himalayan Granite Belt, 24-19 Ma (references in Harrison et al., 1997). Additionally, Harrison et al. (1999) suggest its elliptical shape and small size make it similar to other Northern Himalayan granites. The Mustang Leucogranite is poorly studied as it lies in a limited access area with difficult terrain. These two leucogranite bodies are situated very close to each other and field mapping coupled with remote sensing suggests no obvious boundary between the two.

Tethyan Sedimentary Sequence (TSS)

The Tethyan Sedimentary sequence (TSS) is an approximately 10 kilometer thick Paleozoic - Mesozoic age package of marine carbonate and sedimentary rocks representing the Tethys ocean sediments deposited on the paleo-Indian passive continental margin (Garzanti, 1999) (fig. 3). The TSS lies structurally above the

Figure 3
Stratigraphic column for the Thakkhola Graben modified from Bordet, 1971; Gradstein et al., 1992; Godin et al., 1999b. Column depicts the hanging wall of the Annapurna Detachment consisting of the Tethyan Sedimentary sequence and the Thakkhola Graben basin-fill. The TSS is composed of sequences of sandstone, carbonate, and shale. The basin fill is composed of conglomerates, sandstones, shales, and carbonates. The hanging wall of the Annapurna Detachment is composed of metamorphosed rocks belonging to either the lowermost TSS or the uppermost GHC. The x-axis of the stratigraphic column shows the relative erodability of the units as observed in the field. The units are colored coded according to lithology.

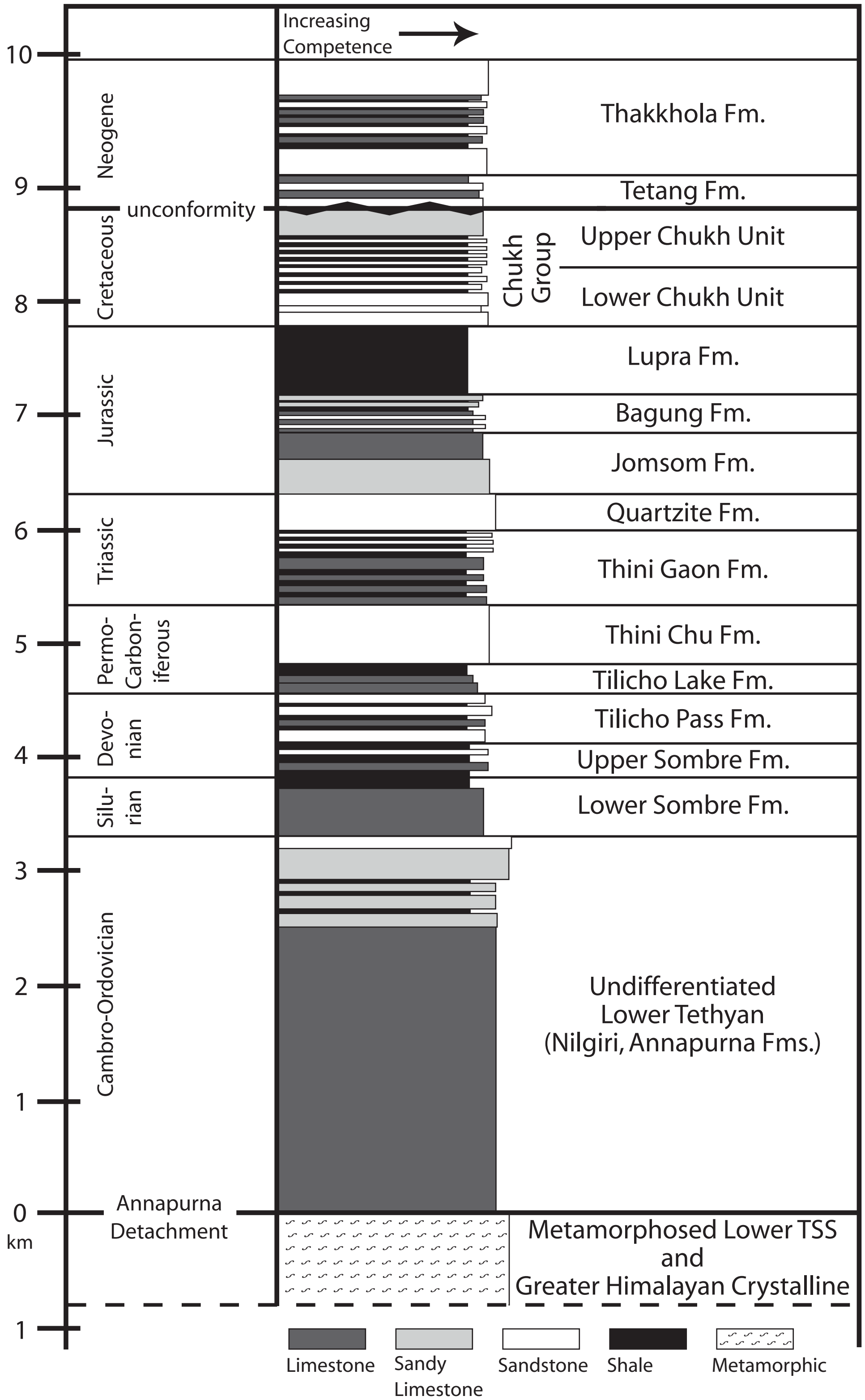

Increasing Competence
10
9
8
7
6
5
4
3
2
1
0
km
1
Neogene
unconformity
Cretaceous
Jurassic
Triassic
Permo-Carbon-iferous
Devo-nian
Silu-rian
Cambro-Ordovician
Annapurna Detachment
Thakkhola Fm.
Tetang Fm.
Chukh Group
Upper Chukh Unit
Lower Chukh Unit
Lupra Fm.
Bagung Fm.
Jomsom Fm.
Quartzite Fm.
Thini Gaon Fm.
Thini Chu Fm.
Tilicho Lake Fm.
Tilicho Pass Fm.
Upper Sombre Fm.
Lower Sombre Fm.
Undifferentiated Lower Tethyan (Nilgiri, Annapurna Fms.)
Metamorphosed Lower TSS and Greater Himalayan Crystalline
Limestone
Sandy Limestone
Sandstone
Shale
Metamorphic

Figure 3

Annapurna Detachment which separates it from higher grade meta-Tethyan and Greater Himalayan rocks intruded by leucogranite dikes and sills below. In the Thakkhola region, no leucogranite bodies have been observed to intrude the TSS above the Annapurna Detachment, as is the case in other studies of the STDS: Machhapuchhare Detachment, Modhi Khola region (Hodges et al., 1996); Qomolangma Detachment, Everest region (Murphy and Harrison, 1999); Phu Detachment, Manaslu region (Searle and Godin, 2003). The TSS has experienced biotite-grade metamorphism at the base and quickly transitions into unmetamorphosed carbonate and sedimentary rocks extensively deformed into kilometer-scale folds (Godin et al., 1999b; Godin, 2003). Stratigraphic thicknesses are represented in figure 3 following Bordet et al. (1971), Colchen et al. (1986), Godin et al. (1999b) with modifications from our own field work.

Paleozoic Tethyan Sedimentary Sequence (TSS)

The oldest portion of the TSS is found at the crest of the Annapurna Range, this is the Cambrian *Sanctuary* Formation; composed of dark graywackes and shales. This formation has been recognized in the Fang Nappe (Pecher, 1978; Colchen et al., 1986) and at the peak of Machhapuchhare (Hodges et al., 1996) where it has been folded into a kilometer scale, recumbent, isoclinal anticline. The *Sanctuary* Formation is interpreted to be in the immediate hanging wall of the STDS (Hodges et al., 1996; Godin et al., 1999b; Searle and Godin, 2003). Owing to the folded nature of both the STDS and the TSS, the *Sanctuary* Formation is no longer observable in the hanging wall north of the Annapurna Range. The overlying Annapurna Formation is more commonly observed in the immediate hanging wall of the STDS (Seale and Godin, 2003). The *Annapurna* Formation consists of calcareous biotite-grade shists and phyllites interlayered with thin low-grade marbles (Godin et al., 1999b). In the Modi Khola region to the west the *Annapurna* Formation has experienced up to amphibolite-grade metamorphism (Hodges et al., 1996). Within the Thakkhola Graben, this formation also contains graphitic schists and phyllites. The *Annapurna* Formation is interpreted to be Cambrian in age (Bordet et al., 1971). The Ordovician age *Nilgiri* Formation, correlative with the *Dhaulagiri Limestone* of Fuchs (1967, 1977), is stratigraphically above the *Annapurna* Formation and consists of massive, blue-gray colored, sparse brachiopod- and nautiloid-bearing carbonate grading upward into rhythmically bedded dolomitic sandstone, calcareous shale, and siltstone. The *Nilgiri* Formation is capped by a 400 meter thick calcareous sandstone and siltstone referred to as the *North Face Quartzite* (Bodenhausen et al., 1964; Bordet et al., 1971; Fuchs, 1988; Garzanti, 1999; Godin et al., 1999b). The Cambrian-Ordovician section is easily observable near the Annapurna and Dhaulagiri Ranges and less extensively within the Thakkhola Graben (Godin et al., 1999b; Godin, 2003; this work). The Silurian-Middle Devonian portion of the TSS section consists of the *Lower* and *Upper Sombre* Formations. The *Lower Sombre* Formation, correlative with the *Dark Band* Formation of Bodenhausen et al. (1964) and Fuchs (1977), consists of cynoid-bearing dolomitic limestone overlain by Early Silurian graptolite-bearing black slates and phyllites. This is overlain by the Early-Middle Devonian *Upper Sombre* Formation which consists of dark limestones, dolomitic quartzarenites, and mudstones containing sparse corals and brachiopods (Bodenhausen et al., 1964; Bordet et al., 1971; Fuchs, 1988; Garzanti, 1999). The Late Devonian stratigraphy is represented by the *Tilicho Pass* Formation. This formation is more fossiliferous than the underlying *Sombre* Formation and consists of gray silty slates with lenses of sandstone, siltstone, and carbonate. The *Tilicho Pass* Formation contains crinoid, conodont, brachiopod, and corral fossils. The sandstone and siltstone beds are frequently rust colored and contain tool marks, flute casts, and burrows; this formation has been interpreted as turbiditic in origin (Bodenhausen et al., 1964; Bordet et al., 1971; Colchen et al., 1986; Fuchs, 1988; Garzanti, 1999). The Carboniferous-Permian section of the TSS is represented by the *Tilicho Lake* and *Thini Chu* Formations. The Early Carboniferous *Tilicho Lake* Formation, correlative with the *Ice Lake* Formation of Bodenhausen et al. (1964), consists of dark gray-blue limestones, calcareous schists, and gray-black shales. This formation contains crinoids, bryozoa, brachiopod, coral, and bivalve fossils (Bodenhausen et al., 1964; Bordet et al., 1967; Fuchs, 1988; Garzanti, 1999). The *Thini Chu* Formation is Middle Carboniferous-Late Permian in age. This formation consists of thickly bedded, medium- to coarse-grained quartzarenites with cross-bedding. The *Thini Chu* Formation is rich in plant and animal fossils and contains a coal layer within the Thakkhola region (Bordet et al., 1971; Bordet et al., 1975).

Mesozoic Tethyan Sedimentary Sequence (TSS)

The Triassic section of the TSS is represented by the *Thini Gaon* and *Quartzite* Formations. Bodenhausen et al. (1964) use the name *Thini Gaon* to broadly label all of the Triassic up to the *Quartzite* Formation, however Fuchs (1967) splits this into three formations; the lowermost being the Lower Triassic *Limestone Band*, followed by the *Mukut Limestone,* and the *Tarap Shales*. The base of the *Thini Goan* Formation is marked by Early Triassic age, rusty weathering, thin bedded, nodular limestone interbedded with thin gray shales. It ranges in color from gray-brown-blue and some beds are rich in ammonites. The middle portion of the *Thini Gaon* Formation, the *Mukut Limestone*, consists of alternating thin bedded, dark gray-blue limestones and shales. The upper portion of the *Thini Gaon* Formation, the *Tarap Shales*, consists of dark gray to green shales interbedded with siltstones and sandstones. This portion contains an abundance of tool marks, flute casts, burrows, and graded beds; it is interpreted to be turbiditic in origin. This gradually alternates between sandstone and shale until the base of the *Quartzite* Formation (Bodenhausen et al., 1964; Fuchs, 1967; Fuchs, 1988). Overlying the *Thini Gaon* Formation is the *Quartzite* Formation which is Latest Triassic in age. The *Quartzite* Formation consists of thickly bedded, fine- to medium-grained sandstones and low-grade metaquartzites. These beds range in color from white-green-brown-pink with bi-directional cross-bedding and burrows commonly observed (Fuchs, 1988). The base of the Jurassic is represented by the *Jomsom* Formation, correlative to the *Kioto Limestone* of Fuchs (1964, 1977, 1988). The *Jomsom* Formation consists of sandy carbonate and shale grading into thick bedded, dark gray-blue limestone and dolomite. The dominantly micritic carbonates contain layers of oolites and fossiliferous packstones and grainstones. Burrowing, cross-bedding, and hummocks have been observed throughout the *Jomsom* Formation (Fuchs, 1988 and Gradstein et al., 1991). Overlying the *Jomsom* Formation is the Middle Jurassic *Bagung* Formation, correlative with the *Lumachelles* Formation of Bodenhausen et al. (1964) and Fuchs (1977). This formation is more thinly bedded than the *Jomsom* Formation and its basal section is comprised of micritic limestone and quartz-rich sandstone grading into a thick calcareous shale unit that alternates with sandy carbonate. Coquina beds are common throughout with evidence of hardground borings. A calcareous sandstone bed is commonly found at the top of the formation (Gradstein et al., 1991). The top of the Jurassic section of the TSS is represented by the *Lupra* Formation

(Bodenhausen et al., 1964 and Bordet et al., 1971), correlative with the *Nupra Shale* of Gradstein et al. (1991) and the *Spiti Shale* of Fuchs (1977). The *Lupra* Formation consists of black shale, rich in nodular concretions ranging from 10s of centimeters to 1-2 meters in diameter. The smaller concretions frequently contain ammonites, which are occasionally pyritized (Gradstein et al., 1991). The Cretaceous is represented by the *Chukh* Group, these are the youngest rocks of the TSS and are only preserved within the Thakkhola Graben (Bodenhausen et al., 1964; Bordet et al., 1971; Fuchs, 1977). This group is composed of four formations, the *Chukh* Formation, *Kagbeni* Formation, *Muding* Formation, and *Dzong* Formation according to the stratigraphy established in Gradstein (1991) and Garzanti (1999). The *Chukh* Formation, correlative to the *Dangardzang* Formation of Garzanti and Frette (1991), is the lowermost portion of the *Chukh* Group and it is comprised of 10-15 meter thick sandstone beds interbedded with very thin siltstone and mudstone. The sandstones are typically glauconitic with sand-sized grains ranging from fine to coarse. Cross-bedding, cross-lamination, and planar laminations are common (Gradstein, 1991). The *Kagbeni* Formation, correlative with the *Dzong (a)* of Garzanti and Frette (1991), consists of greenish colored sandstone, siltstone, and mudstone. The sandstone beds are up to 10 meters thick and composed dominantly of volcanic grains that are fine- to medium-grained, occasionally granule- to pebble-sized (Gradstein, 1991). Wood fragments and coal have been observed in this formation (Garzanti and Frette, 1991). The *Muding* Formation, correlative with the *Dzong (b)* of Garzanti and Frette (1991), overlies the *Kagbeni* Formation and consists of dark brown shale interbedded with thin, white-green glauconitic sandstones. The sandstones are frequently erosionally based and some contain ammonite and bivalve fossils. The uppermost *Chukh* Group consists of the *Dzong* Formation, correlative with the *Muding* Formation of Garzanti and Frette (1991). This formation consists of thin-bedded, pale marlstone and silty limestone. Uncommon thin glauconitic beds are observed as well (Gradstein, 1991). For the purpose of field mapping, we divided this group into the *Lower Chukh* Unit and *Upper Chukh* Unit. The *Lower Chukh* Unit consists of the basal *Chukh* Formation and overlying *Kagbeni* Formation, the *Upper Chukh* Unit consists of the *Muding* Formation and overlying *Dzong* Formation.

Basin-fill Sediment

The sedimentary fill of the Thakkhola Graben has been deposited in buttress unconformity on top of the deformed TSS and is divided into the *Tetang* Formation and overlying *Thakkhola* Formation (fig. 3). These two formations contain sediment derived from the eroded western and eastern footwalls as well as material brought in from the north via the southward flowing Kali Gandaki. The *Tetang* and *Thakkhola* Formations have been studied in detail by Garzione et al. (2003) using correlated measured sections coupled with abundant clast counts and paleocurrent analyses. They describe these formations as consisting of three alternating lithofacies; alluvial fan, braided stream, and lacustrine. The *Tetang* Formation was deposited as early as 11 Ma based upon magnetostratigraphy and generally contains clasts derived from the eastern footwall. The *Thakkhola* Formation was deposited after 7 Ma based upon C_4 grasses found within a paleosol; it generally contains clasts derived from the western footwall and from Tibet to the north (Garzione et al., 2000; Garzione et al., 2003). There is a 5^{o} angular unconformity between these formations due to the underyling *Tetang* Formation having been rotated towards the west prior to deposition of the *Thakkhola* Formation; an approximately 2.6 m.y. age gap is observed between the two (Garzione et al., 2003).

Tetang Formation

The *Tetang* Formation is approximately 240 meters thick and found around Tetang Village near the center of the graben. The lower portion of the *Tetang* Formation consists of alluvial fan and braid-stream deposits. Braided stream deposits are more common towards the center of the basin, suggesting an axial drainage during the time of deposition. Alluvial fan deposits are concentrated on the edges of the basin, suggesting steep gradients had already been developed along the margins of the basin (Garzione et al., 2003). The *Tetang* Formation has been divided into four units according to Bassoullet and Colchen (1974). Unit I, the basal unit, consists of pebble and gravel conglomerates composed mostly of quartzite clasts and is up to 35 meters thick. These conglomerates are clast supported and contain a minor matrix component of orange-white sand- and silt-sized grains. Unit II, up to 70 meters thick, contains meter-thick limestone beds interbedded with pebble and gravel conglomerates, much like those of Unit I. Inverse grading as well as trough cross-stratification have been observed in some of the conglomerate beds of Unit II. The limestone beds are gray-tan colored and micritic with some minor evidence of roots and other plant matter. Unit III consists of clast supported, pebble conglomerates composed mainly of leucogranite clasts mixed with a minor component of TSS and is approximately 100 meters thick. Unit IV, approximately 50 meters thick, is mainly composed of thin sandstones and calcareous shales.

Thakkhola Formation

The *Thakkhola* Formation is approximately 800 meters thick and decreases in thickness towards the east. Deposition of the *Thakkhola* Formation is much more widespread than for the *Tetang* Formation, spanning approximately 20-30 kilometers across the basin and approximately 40-60 kilometers along the basin (Colchen, 1999). The *Thakkhola* Formation consists of alluvial fan and braided-stream deposits grading into lacustrine limestones capped by thin sandstones and conglomerates. This formation has been divided into three units by Bassoullet and Colchen (1974). Unit I, up to 150 meters thick, is found at the base and consists of clast supported pebble and cobble conglomerates composed of metamorphosed TSS and leucogranites. The metamorphosed TSS clasts are interpreted to represent structurally deeper portions of the TSS exposed after significant displacement in the graben-bounding faults. Unit II, up to 300 meters thick, contains meter-thick lenses of sandstone and pebble conglomerate with lacustrine limestone and calcareous mudstone. The conglomerate clasts are typically metamorphosed TSS and leucogranites. The limestone is white-gray-tan, massive, micritic limestone. Plant matter is common in the limestone beds. The sandstones consist of fine sand- to silt-sized quartz and feldspar grains which contain sparse pebbles similar in composition to the surrounding conglomerates. Unit III is approximately 200 meters thick and consists of thin sandstones and conglomerates. The conglomerate clasts are pebble- and cobble-sized and composed of metamorphosed TSS and leucogranite.

Thakkhola Graben

The Thakkhola Graben is bounded by two steeply dipping, ~N20^{o}E – N40^{o}E-striking normal faults; the Dangardzang Fault to the west and the Muktinath Fault to the east. The northern and southern boundaries have been interpreted to be near the Indus-Yalu Suture and within the footwall of the Annapurna Detachment, respectively. Both bounding faults are observable as far south as the crest of the High Himalayas; the Dangardzang Fault is traceable for about 100 kilometers north to the Indus-Yalu Suture and the Muktinath Fault is traceable for about 50 to 70 kilometers to the north. The graben's width tapers from approximately 30 kilometers in the north to less than 5 kilometers in the south (Gansser, 1964; Bordet et al., 1975; Colchen, 1999; Hurtado et al., 2001; Godin, 2003) (figs. 1 and 2,). In addition to the graben-bounding faults, two faults have been observed which strike orthogonal to the trend of the graben; they are the Lupra Fault (Colchen et al., 1986; Godin, 2003) and the Kagbeni Fault (this work) (fig. 2). The Kagbeni Fault runs across the basin into both the eastern and western footwalls and has been observed to be offset by the Dangardzang and Muktinath Faults (this work). Therefore it must predate movement on either fault. The Lupra Fault runs from the western footwall of the graben into the middle of the basin and is not observed to be offset along the Dangardzang Fault (Godin et al., 2003). This implies the Lupra Fault is younger than the motion on the Dangardzang Fault.

In the summer of 2009 and 2010 field work was conducted within the graben over an area approximately 50 kilometers north-south by 30 kilometers east-west. This field work resulted in a 1:50,000 scale geologic map of the central portion of the Thakkhola Graben (fig. 4). In addition to this field map we have used SRTM elevation data to

Figure 4
Geologic map of the Thakkhola Graben (1: 50,000 scale) modified from Colchen et al., 1981; Godin et al., 2003. Depicts the Dangardzang Fault and the Muktinath Fault bounding the western and eastern side of the basin, respectively. TSS rocks found in the graben footwalls folded into WNW-ESE striking anticlines and synclines. The basin-fill rocks have been deformed into NNE-SSW striking folds. Dangardzang and Muktinath Faults cut and offset the folded TSS, Kagbeni Fault, and potentially the Mustang Detachment. The Lupra Fault does not appear to be offset along the Dangardzang Fault. Locations for cross-sections A-A′, B-B′, C-C′, and D-D′ are depicted on the map.

Figure 4

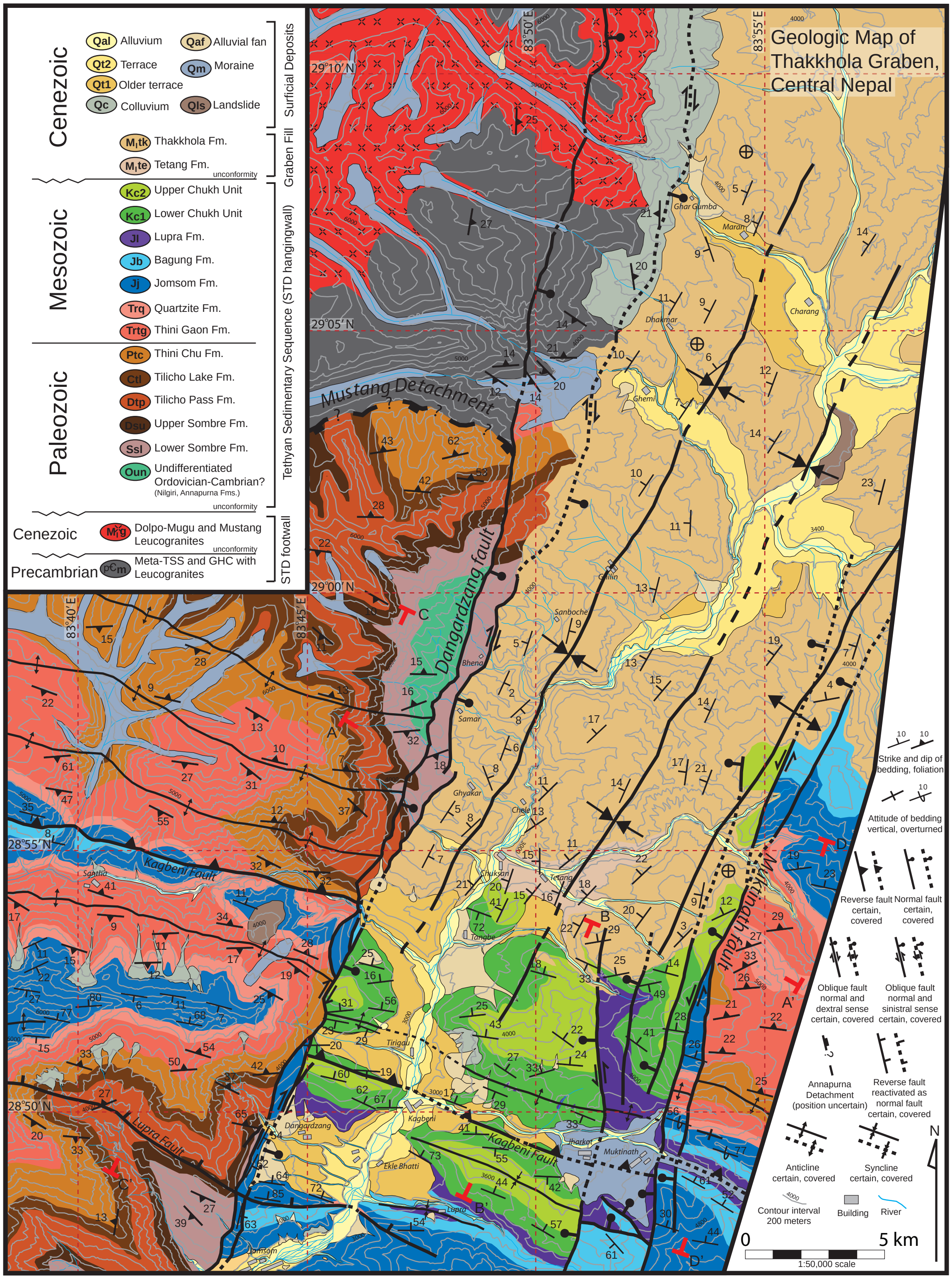
Geologic Map of Thakkhola Graben, Central Nepal
Cenezoic
Qal Alluvium
Qaf Alluvial fan
Qt2 Terrace
Qm Moraine
Qt1 Older terrace
Qc Colluvium
Qls Landslide
Surficial Deposits
M1tk Thakkhola Fm.
M1te Tetang Fm.
unconformity
Graben Fill
Mesozoic
Kc2 Upper Chukh Unit
Kc1 Lower Chukh Unit
Jl Lupra Fm.
Jb Bagung Fm.
Jj Jomsom Fm.
Trq Quartzite Fm.
Trtg Thini Gaon Fm.
Paleozoic
Ptc Thini Chu Fm.
Ctl Tilicho Lake Fm.
Dtp Tilicho Pass Fm.
Dsu Upper Sombre Fm.
Ssl Lower Sombre Fm.
Oun Undifferentiated Ordovician-Cambrian?
(Nilgiri, Annapurna Fms.)
unconformity
Tethyan Sedimentary Sequence (STD hangingwall)
Cenezoic
Dolpo-Mugu and Mustang Leucogranites
unconformity
Precambrian
Meta-TSS and GHC with Leucogranites
STD footwall
Mustang Detachment
Dangardzang fault
Kagbeni Fault
Lupra Fault
Muktinath fault
29°10'N
29°05'N
29°00'N
28°55'N
28°50'N
83°40'E
83°45'E
83°50'E
83°55'E
Ghar Gumba
Maran
Charang
Dhakmar
Ghemi
Gillin
Sanboche
Bhena
Samar
Ghyakar
Chele
Chuksan
Tetang
Tangbe
Tiriqau
Kagbeni
Dangardzang
Ekle Bhatti
Lupra
Jharkot
Muktinath
Jomsom
Sangda
A
A'
B
B'
C
D
D'
Strike and dip of bedding, foliation
Attitude of bedding vertical, overturned
Reverse fault certain, covered
Normal fault certain, covered
Oblique fault normal and dextral sense certain, covered
Oblique fault normal and sinistral sense certain, covered
Annapurna Detachment (position uncertain)
Reverse fault reactivated as normal fault certain, covered
Anticline certain, covered
Syncline certain, covered
Contour interval 200 meters
Building
River
N
0
5 km
1:50,000 scale

produce a map of the northernmost portion of the Thakkhola Graben based on offset ridges and fault scarps (fig. 8). We mapped a 50-kilometer segment of the Dangardzang Fault and a 30-kilometer segment of the Muktinath Fault. In addition to the graben-bounding faults, this map depicts the locations and attitudes of several structural and geological features; intensely folded Tethyan rocks in both graben footwalls, broadly folded basin-fill sediment, the graben-perpendicular Lupra and Kagbeni Faults, the Dolpo-Mugu and Mustang Leucogranites in the northern portion of the Dangardzang footwall, and a previously unrecognized structural boundary termed the Mustang Detachment. Field work was carried out in the basin and both footwalls in order to determine the attitude and position of the basin-fill and Tethyan formations. This field work has been used to produce 4 cross-sections; 1 in the footwall of the Dangardzang Fault (fig. 5a), 1 in the footwall of the Muktinath Fault (fig. 5b), 1 perpendicular to the basin (fig. 10a), and 1 parallel to the basin (fig. 10b).

Dangardzang Fault Footwall

The footwall of the Dangardzang Fault is found on the western side of the mapping area (fig. 4) and represented in cross-section C-C' (fig. 5a), the northernmost portion of this footwall is shown in figure 8. The following description is from south to north. Just south of the Lupra Fault, the Dangardzang footwall is composed of Middle Paleozoic Tethyan rocks; the deepest being the *Lower Sombre* Formation and as young as the uppermost portions of the *Thini Gaon* Formation. These rocks on the ridge leading up to the Lupra Fault, just west of Jomsom Village, comprise the northern limb of a north-vergent syncline (fig. 5a). The ~ 300-290^{o}-striking Lupra Fault is found on the slope northwest of Jomsom (fig. 4). At this location the fault cuts through the Tethyan

Figure 5a
Cross-section C-C' is oriented parallel to the Dangardzang Fault in the western footwall of the Thakkhola Graben. The southern portion of the section is modified from Godin, 2003. The Lupra Fault is interpreted to be a reverse fault reactivated as a normal fault during the final stage of graben development. The Kagbeni Fault separates north-verging folds from south-verging folds and is intepreted to have formed prior to the development of the graben. The folds, Kagbeni Fault, and Lupra Fault are interpreted to root into the brittle Annapurna Detachment (AD). ASZ - Annapurna Shear Zone.

Figure 5b
Cross-section D-D' is oriented parallel to the Muktinath Fault in the eastern footwall of the Thakkhola Graben. The Kagbeni Fault strikes parallel to Thorung La Valley separating the south-verging anticline on Thorung North peak from the upright to north-verging anticline on Thorung South peak. AD - Annapurna Detachment, ASZ - Annapurna Shear Zone.

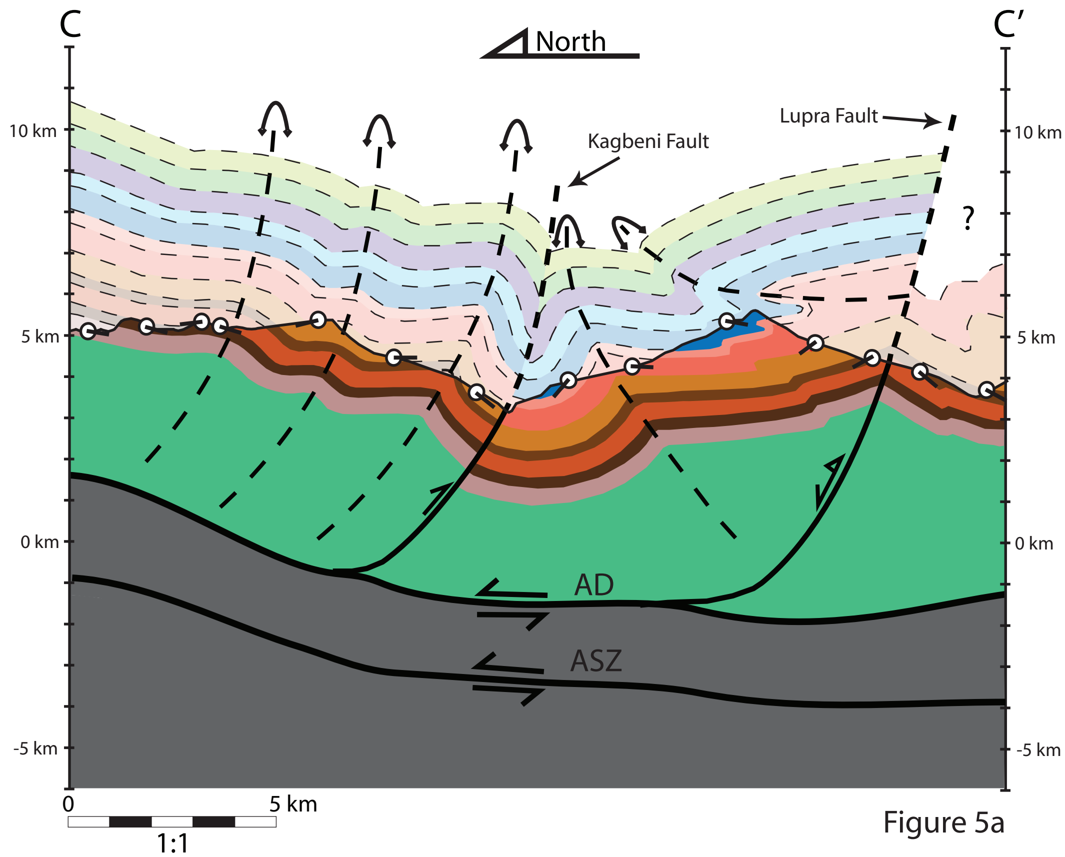

Figure 5a

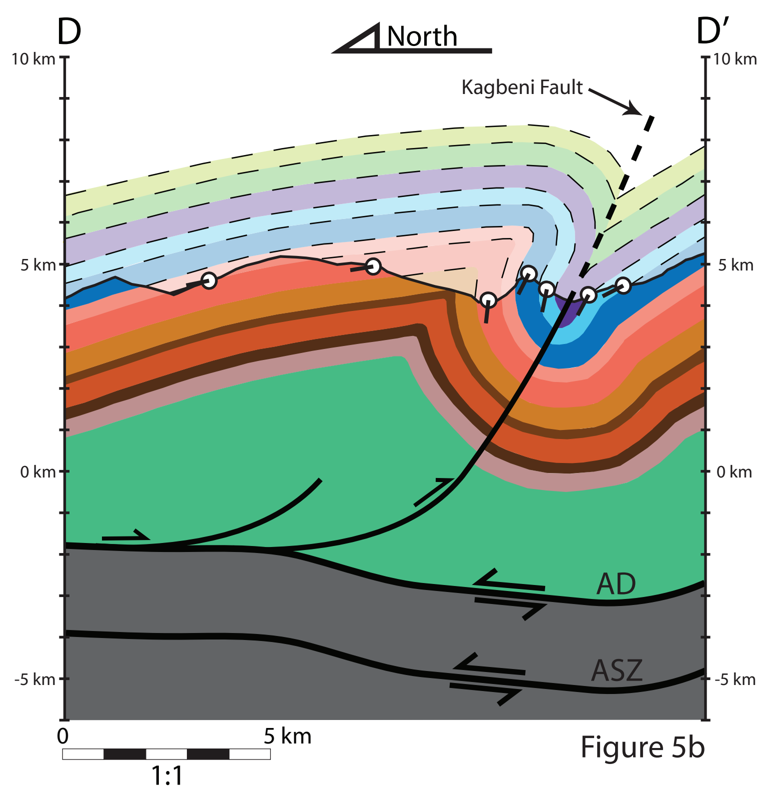

Figure 5b

sedimentary rocks but expresses no discernible stratigraphic offset. There is a change in dip direction from the footwall (~ 30^o SW) to the hanging wall (~ 30^o NE) of the Lupra Fault (fig. 6a). Fold axial planes are not traceable across this fault as is shown in the cross-section at around 6000 meters along the Lupra Fault (fig. 5a). The nearly horizontal axial plane within the Thini Gaon at this elevation has been transferred from an adjacent cross-section in Godin (2003) where the author observes that the axial planes of folds cannot be matched on either side of the Lupra Fault. North of the Lupra Fault, Middle Paleozoic through Middle Mesozoic Tethyan rocks make up the southern slope of Dangar Ridge (figs. 4 and 5a). The crest of this ridge is composed of the Jurrassic *Jomsom* Formation that has been folded into a tight, north-vergent anticline-syncline pair (figs. 4, 5a, and 7a,b) with an axial plane attitude of 097^o/13^o S (fig. 6b). The *Jomsom* Formation comprises the ridge crest as well as a portion of the northern slope down to about 4000 meters. This thick exposure is facilitated partially by the near parallelism of the northern slope (~ 30^o) with the dip of the *Jomsom* Formation (10-25^o N) (fig. 5a). This is also facilitated by a parasitic syncline at 5000 meters of elevation (fig. 5a). Moving down slope the *Quartzite* and *Thini Gaon* Formations are exposed in a north-vergent anticline with an interlimb angle of about 90^o and an axial plane attitude of ~ N65^{o}W, 50^o SW (figs. 4 and 5a). The *Jomsom* Formation is again exposed as the northern limb of the anticline intersects the ground. Down slope and towards Santha Village the dips change from ~ 30-40^o NE to about 10^o NE as the rocks are smoothly folded (figs. 5a and 6c). The *Bagung* Formation is exposed on the cliffs just north of Santha Village marking the youngest TSS rocks in the Dangardzang footwall (fig. 4). A steeply dipping and 295^o-striking reverse-sense fault is observed north of Santha (fig. 4)). East of Santha Village

Figure 6

Stereplots representing the orientation of the folded rocks in the footwall of the Dangardzang Fault. All stereoplots are equal area and projected in the lower hemisphere. The description is from south to north with the planar attitudes represented above the pole concentrations. Stereoplot A - the Lupra Fault cuts and offsets an upright, slightly north-verging anticline. Stereoplot B - Tasartse peak, immediately south of Santha Village, contains an almost isoclinally folded anticline-syncline pair that verges strongly to the north. Stereoplot C - the rocks on either side of the Kagbeni Fault dip towards each other forming an upright isoclinally folded syncline in the *Lupra* shale. Stereoplot D - further into the hanging wall of the Kagbeni Fault the rocks are folded into a train of south-verging anticlines and synclines. Stereoplot E - the rocks within the immediate Mustang Detachment hanging wall are part of a south-verging anticline. The northern limb dips steeply towards the detachment. Stereoplot F - the rocks in footwall of the Mustang Detachment exhibit homoclinal dips with much smaller scale folding than the rocks in the hanging wall.

Figure 6

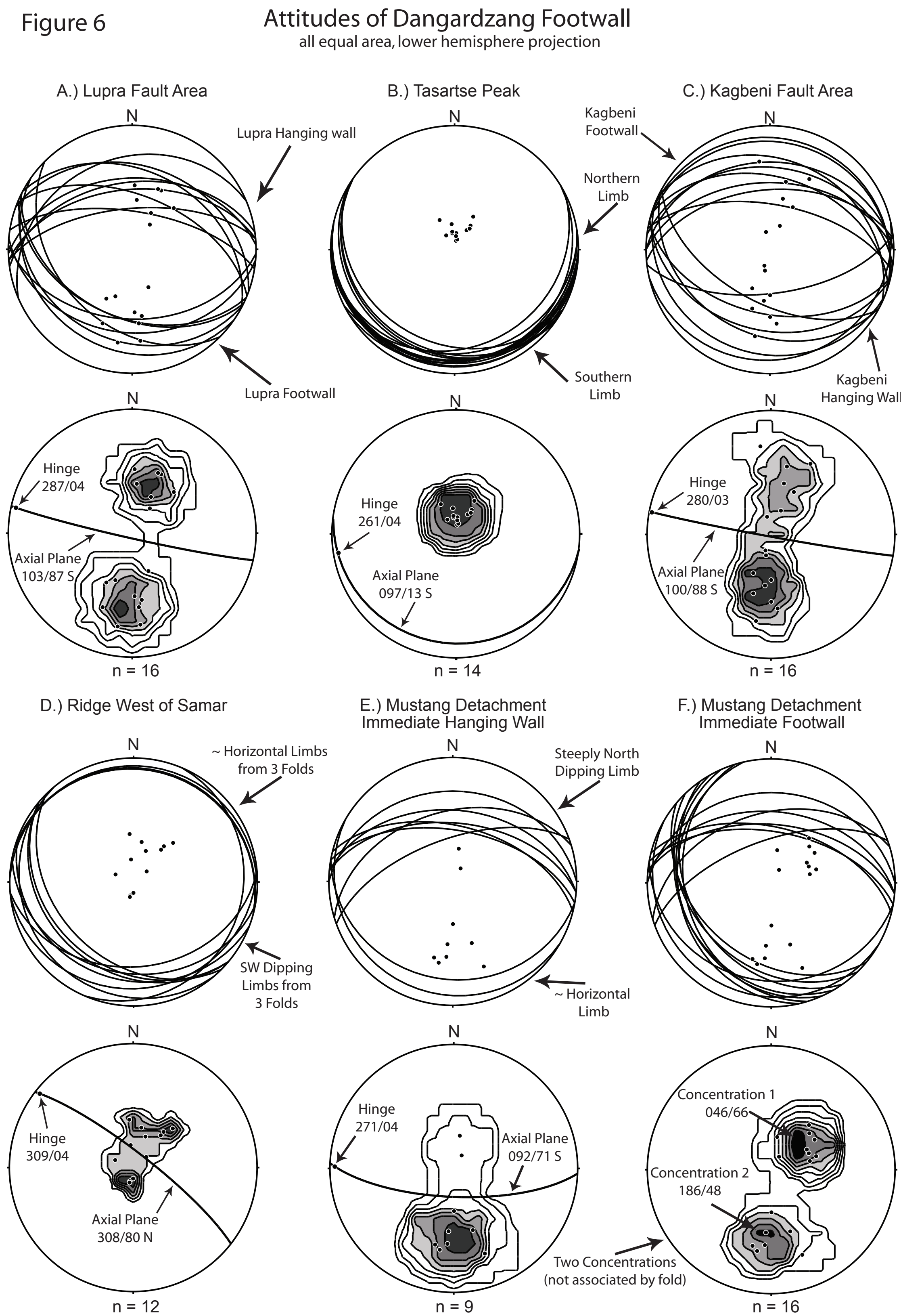

Attitudes of Dangardzang Footwall
all equal area, lower hemisphere projection
A.) Lupra Fault Area
N
Lupra Hanging wall
Lupra Footwall
N
Hinge
287/04
Axial Plane
103/87 S
n = 16
B.) Tasartse Peak
N
Northern
Limb
Southern
Limb
N
Hinge
261/04
Axial Plane
097/13 S
n = 14
C.) Kagbeni Fault Area
N
Kagbeni
Footwall
Kagbeni
Hanging Wall
N
Hinge
280/03
Axial Plane
100/88 S
n = 16
D.) Ridge West of Samar
N
~ Horizontal Limbs
from 3 Folds
SW Dipping
Limbs from
3 Folds
N
Hinge
309/04
Axial Plane
308/80 N
n = 12
E.) Mustang Detachment
Immediate Hanging Wall
N
Steeply North
Dipping Limb
~ Horizontal
Limb
N
Hinge
271/04
Axial Plane
092/71 S
n = 9
F.) Mustang Detachment
Immediate Footwall
N
N
Concentration 1
046/66
Concentration 2
186/48
Two Concentrations
(not associated by fold)
n = 16

the trace of the fault trends downhill towards the valley and to the west it trends uphill (fig. 4). This fault, referred to as the Kagbeni Fault, is top-to-the-south and expresses about 500-700 meters of vertical displacement (fig. 5a). In the Dangardzang footwall this fault appears to be a structural boundary separating north-vergent folding to the south from upright or south-vergent folding to the north (figs. 5a and 6a-d). On the basis of fault plane attitude and position relative to surrounding structures we interpret this fault to be a western continuation of the reverse fault depicted in the Kagbeni structure of Godin (2003). The trace of the Kagbeni Fault is cut and offset along the Dangardzang Fault with ~6.5 kilometers of right lateral separation (fig. 4). The slope north of Santha Village is dominantly covered by the *Thini Chu* and *Thini Gaon* Formations that have been folded several times into several upright to slightly south-vergent syncline-anticline pairs, (figs. 4 and 5a) (syncline symbols omitted for space). These folds have steeply dipping axial planes, ~ 80^{o} NE, with strikes of ~ 308^{o} (fig. 6d). The southernmost of these, at 4000 meters elevation in cross-section C-C', has an interlimb angle of nearly 90^{o} and the rest of the folds are closer to 120^{o} (fig. 5a). The deepest TSS rocks exposed in the mapping area are found to the west of the villages of Samar and Bhena (fig. 4). This is mapped as the undifferentiated Cambrian-Ordovician, most likely the *Nilgiri* Formation, consisting of low-grade, blue-gray marble and fine-grained sandstone. North of the 29^{0} 00'N line the *Tilicho Pass* Formation makes up the crest of an east-west-trending ridge (fig. 4). Moving northward the ridge turns towards the NNE and the dip direction changes from south to north. The dip angle also changes from ~30^{o} -45^{o} N, even as steep as 62^{o} N (figs. 4 and 6e). At about 5400 meters of elevation a major structural and metamorphic discontinuity has been recognized. Above this discontinuity are the unmetamorphosed

Figure 7
A - view looking west along Syang Khola towards the south side of Tastartse peak. This peak is composed of an isoclinally folded, steeply north-verging anticline-syncline pair (Dangardzang footwall). B - view of the north side of Tasartse peak where the steeply north-verging anticline is shown to be continuous along the ridge to the east (Dangardzang footwall). C - view of Thorung La pass. Thorung North peak is composed of a steeply south-verging anticline and Thorung South peak is composed of an upright to slightly south-verging anticline (Muktinath footwall). D - view within the Thakkhola Graben basin showing regionally continuous dip panels in the basin fill units. These dip panels make up the limbs of north-south trending, gently folding anticlines and synclines.

Figure 7

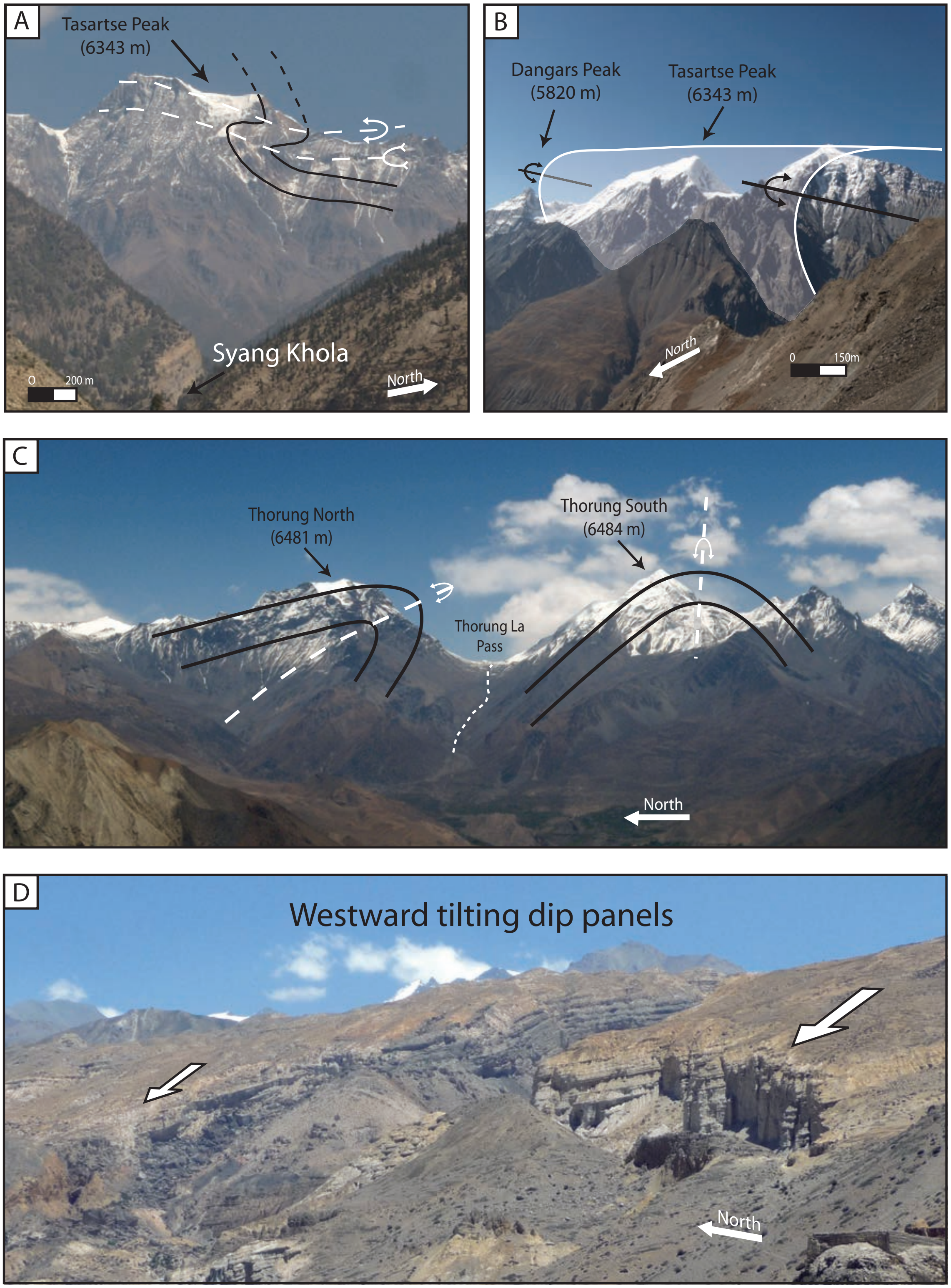

A
Tasartse Peak
(6343 m)
Syang Khola
0
200 m
North
B
Dangars Peak
(5820 m)
Tasartse Peak
(6343 m)
North
0
150m
C
Thorung North
(6481 m)
Thorung South
(6484 m)
Thorung La
Pass
North
D
Westward tilting dip panels
North

Middle-Late Paleozoic Tethyan rocks and below this discontinuity are metamorphic rocks more akin to the GHC than the TSS. The metamorphic rocks consist of garnet staurolite schist, biotite schist, garnet biotite schist, and calc-silicate gneiss all pervasively intruded by leucogranite dikes and sills showing extensive deformation. Coincident with the metamorphic discontinuity is a change from folded TSS above to shallowly dipping (>30^{o}), nearly homoclinal metamorphic rocks (fig. 4 and 6c). Without further analysis it is impossible to tell whether these are GHC rocks or metamorphosed TSS rocks and as such they have been mapped as undifferentiated meta-TSS and GHC with leucogranites. This discontinuity has been named the Mustang Detachment and it appears to be similar in style and structural position to the Phu Detachment of Searle and Godin (2003) (fig. 2). The contacts of the TSS are truncated against the Mustang Detachment, implying a ramp relationship with the fault (fig. 4). Direct observation of the detachment surface was not possible, and as such its position is approximate. The northwest corner of the mapping area in figure 4, southwest portion of figure 8, is composed of leucogranite surrounded by metamorphosed Cambrian-Ordovician TSS or the uppermost formations of the GHC. These leucogranites have been described by previous authors as consisting of two granitic bodies; the Dolpo-Mugu and the Mustang Leucogranites (Colchen et al, 1986; Le Fort and France-Lanord, 1995; Harrison et al., 1999, Hurtado et al., 2001). The boundary between the Dolpo-Mugu and Mustang Leucogranites has been placed along the northwest-trending valley that runs through the villages of Charang and Maran (Colchen et al., 1986; Hurtado et al., 2001). Our field mapping, combined with analysis of Aster data and Google Earth imagery, reveals no clear boundary within this valley (figs. 4 and 8). The valley floor has a thick accumulation of glacial till but the valley walls are

Figure 8
Map of the northern half of the Thakkhola Graben. The Dangardzang Fault cuts and offsets the Mustang Leucogranite and potentially the Mustang Detachment. The Dangardzang Fault consists of two faults with oblique dextral strike-slip faulting occuring on the eastern fault and normal dip-slip occuring on the western fault. In this portion of the graben the Muktinath Fault consists of two strands with oblique sinistral strike-slip faulting occuring on the western fault and normal dip-slip faulting occuring on the eastern fault.

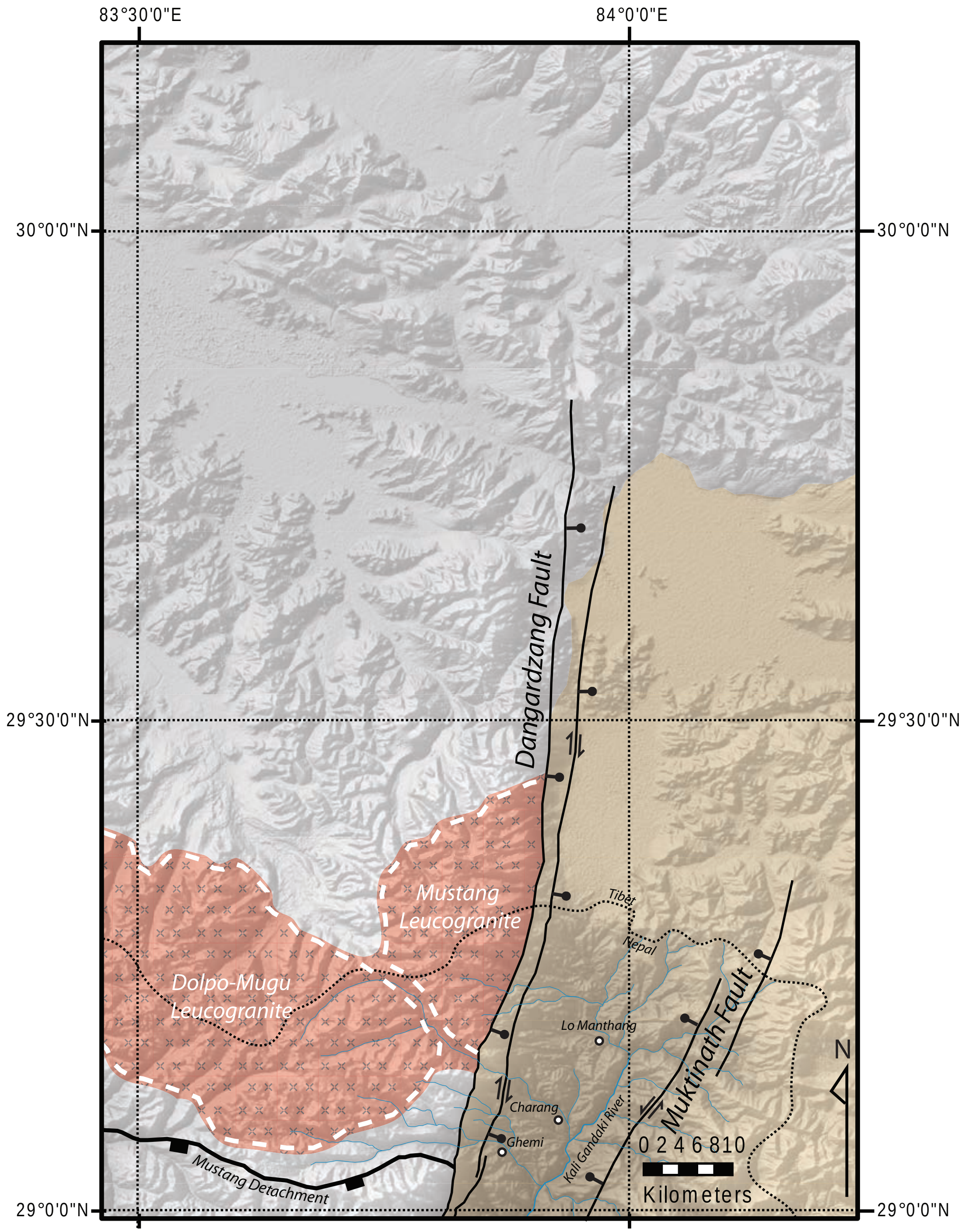
83°30'0"E
84°0'0"E
30°0'0"N
29°30'0"N
29°0'0"N
Dangardzang Fault
Mustang Leucogranite
Dolpo-Mugu Leucogranite
Tibet
Nepal
Lo Manthang
Muktinath Fault
Charang
Ghemi
Kali Gandaki River
Mustang Detachment
0 2 4 6 8 10
Kilometers
N

Figure 8

composed of leucogranite bedrock that appears to be in place. There are no apparent intervening structures or lithologies. Because of this we have mapped the Dolpo-Mugu and Mustang Leucogranites as a continuous leucogranite body, with the Mustang Leucogranite being a north-trending arm of the much larger east-west-trending Dolpo-Mugu Leucogranite. Geochemical analysis and additional field work are necessary to more adequately differentiate these bodies. The footwall of the Dangardzang Fault at the northern boundary of figure 4 is comprised of the Mustang portion of the leucogranite capped by a few hundred meters of calcareous schist and garnet-biotite gneiss. The Mustang Leucogranite extends for another 30 kilometers north of figure 4 and at most 15 kilometers west of the Dangardzang Fault (fig. 8). It is possible to follow the trace of the Dangardzang Fault until it runs into a 10 kilometer wide, northwest-trending valley at approximately 30^{o} North (fig. 8).

Muktinath Fault Footwall

The footwall of the Muktinath Fault comprises the southeast corner of figure 4 and is represented in cross-section D-D’ (fig. 5b). This portion of the map depicts the TSS rocks surrounding the east-west-trending Thorung La Valley to the east of Muktinath Village (figs. 2 and 4). The peaks of Thorung North and Thorung South (fig. 2), located north and south of Thorung La Valley, respectively, are composed of Mesozoic Tethyan rocks folded into 2 kilometer-scale anticlines with a tight syncline in the intervening valley (figs. 4, 5b, and 7) (Colchen et al., 1981). The southeastern portion of figure 4 begins on the northern slope of Thorung South. This slope is the dip surface of the northern limb of a slightly south-vergent antlicline with an axial plane attitude of 293^{o}/85^{o} N (fig. 9a). Close to the peak the northern limb of the Thorung South anticline is

Figure 9
Stereoplots representing the orientation of the folded rocks in the footwall of the Muktinath Fault (A and B) and the orientation of the folded Tethyan rocks in the Thakkhola Graben basin (C and D). All stereoplots are equal are and projected in the lower hemisphere. A - Thorung South peak is composed of an upright to slightly south-verging anticline. B - Thorung North peak is composed of strongly south-verging anticline. C - the footwall rocks of the Kagbeni Fault are deformed into an upright to slightly north-verging syncline. D - the hanging wall rocks of the Kagbeni Fault are deformed into a south-verging anticline.

Figure 9

Attitudes of Muktinath Footwall

all equal area, lower hemisphere projection

A.) Thorung South Anticline

B.) Thorung North Anticline

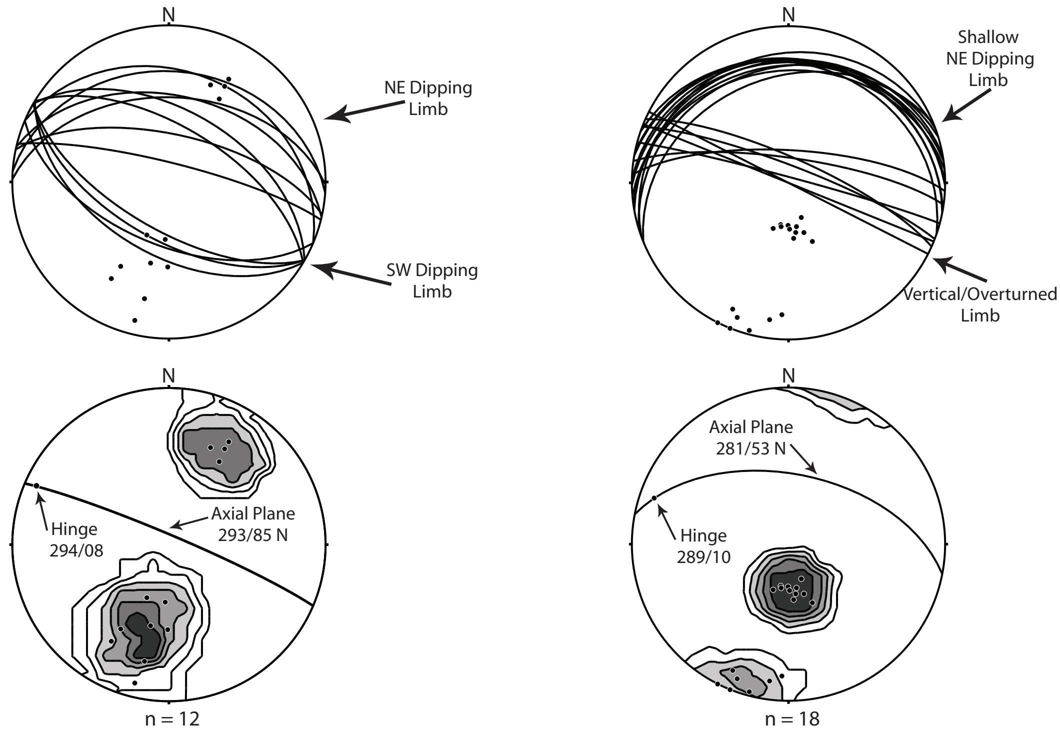

Attitudes of Basin Tethyan Units

all equal area, lower hemisphere projection

C.) Syncline in Footwall of Kagbeni Fault

D.) Anticline in Hanging Wall of Kagbeni Fault

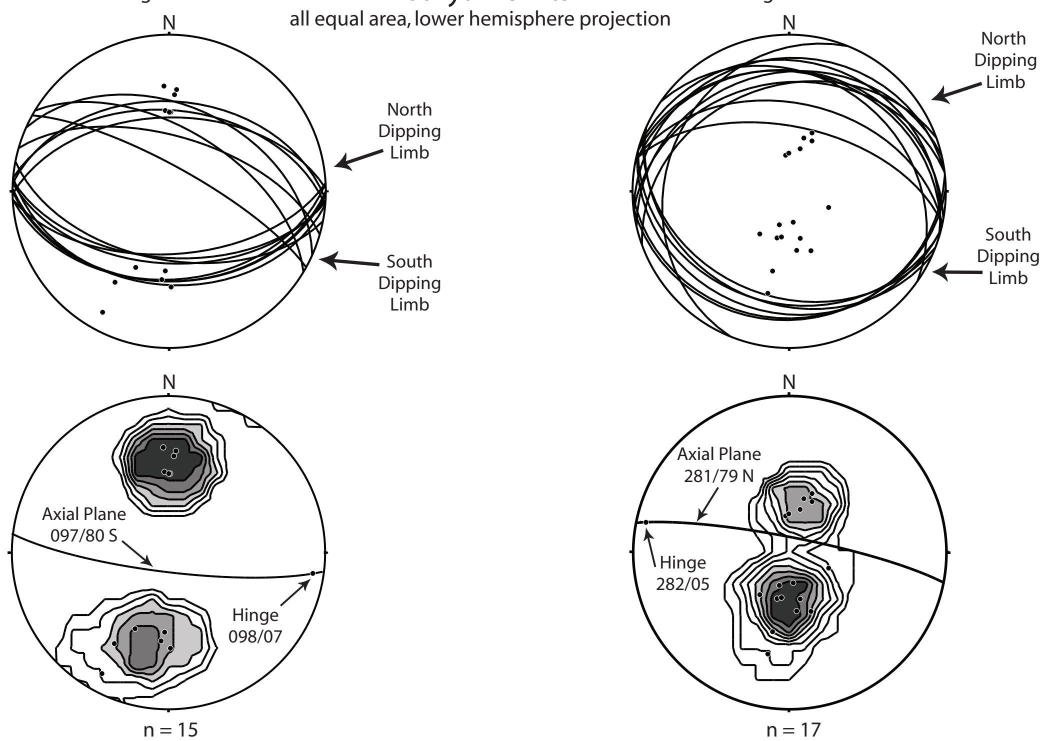

composed of the *Jomsom* Formation and younger formations, *Bagung* and *Lupra*, are exposed in regular stratigraphic succession towards the valley (fig. 4 and 5b). This northern limb shows an abrupt increase in dip angle from 30-44^{o} NE near the hinge to as steep as 61^{o} NE near Thorung La Valley (figs. 4, 5b). Thorung La Valley is composed of the *Lupra* Formation with both adjacent valley walls being composed of the *Bagung* Formation (figs. 4 and 5b). The Tethyan rocks within the valley have been folded into a south-vergent syncline with an isoclinal interlimb angle; this fold has been cut by a steeply north-dipping, reverse-sense fault (fig. 5b). On the basis of the fault plane attitude as well as its position relative to surrounding folds we interpret this fault to be the continuation of the Kagbeni Fault found in the Dangardzang Fault footwall. The top-to-the-south Kagbeni Fault strikes ~300^{o} and runs parallel to Thorung La Valley beneath an accumulation of glacial sediment. Towards Muktinath Village the trace of the fault is observed to be offset ~ 1 kilometer along the Muktinath Fault with an apparent sinistral sense (fig. 4). The *Lupra* through *Jomsom* sequence is repeated moving north of Thorung La Valley into the southernmost ridge of Thorung North. The rocks which comprise this ridge are overturned and very steeply dipping representing the southern limb of the Thorung North anticline (figs. 4 and 5b). The Thorung North anticline is south-vergent with an axial plane attitude of 281^{o}/53^{o} N (fig. 9). Coincident with observations in the Dangardzang Fault footwall, the Kagbeni Fault again appears to be a structural boundary separating south-vergent folds to the north from north-vergent or upright folds to the south (figs. 5b and 7c). Moving towards Tangarghiu Valley, the small valley immediately north of Thorung La Valley, the southern limb of the Thorung North anticline changes from steeply overturned to vertical and the rocks become progressively older towards the trace of the axial plane (figs. 4 and 5b). The southern wall of Tangarghiu Valley is composed of vertical slabs of the Mesozoic *Quartzite* Formation. The oldest Tethyan rocks in the Muktinath Fault footwall, the *Thini Chu* Formation, and the trace of the axial plane for the Thorung North anticline are located on the northern wall of Tangarghiu Valley (fig. 4). The trace of the axial plane appears to be offset along the Muktinath Fault with a sinistral sense and the *Thini Chu* Formation is only found in the easternmost hanging wall within the core of the anticline (fig. 4). To the north of the Tangarghiu Valley the western slope of Thorung North is composed dominantly of the *Thini Gaon* Formation. The rocks making up this portion of Thorung North have a consistent dip of ~ 25^{o} NW (figs. 4, 5b, and 9b). The *Quartzite* Formation crops out again at 5100 meters on the crest of the northwest-trending ridge that makes up the southern wall of the Yakchnu Valley, the next valley to the north (figs. 4 and 5b). This valley contains a small portion of the basin-fill *Thakkhola* Formation lying unconformably on the *Thini Gaon* Formation. The ridges north of Yakchnu Valley are composed of a continuous, upright stratigraphic section of TSS up to the *Bagung* Formation (figs. 4 and 5b). These rocks are dipping consistently ~20^{o} NW (figs. 4, 5b, and 9b). Basin-fill sediment covers the northern portion of the Muktinath Fault footwall (fig. 4).

Tethyan Fold Interpretation

Godin (2003) describes several deformational phases responsible for the structures observed within the Tethyan rocks: (D1) initial south-verging folds, (D2) north-verging back folding, (D3) shear associated with the Annapurna Detachment, (D4) south-verging compressional deformation, and (D5) the development of the Thakkhola Graben. Within our field area fold orientations change from north-vergent to upright or south-vergent from the southern boundary to the north. North-vergent folds observed on Dangarz and Tastartse peaks (figs. 7a,b) are associated with the D2 phase of deformation. Upright folds such as the one comprising Thorung South may have initially been north-vergent and were reoriented during D4 south-vergent compression. South-vergent folds such as the Thorung North anticline and those others found north of the Kagbeni Fault are associated with the D4 south-vergent compressional phase of deformation. The transition from north- to south-vergent folds suggests the intensity of D2 north-vergent back folding diminishes towards the north allowing D2 folds in the northern portion of the mapping area to be reoriented during D4.

Thakkhola Graben Basin

The width of the Thakkhola Graben varies from approximately 5 kilometers around the Annapurna Detachment to as much as 25-30 kilometers in Tibet to the north (figs. 2, 4, and 8) (Colchen, 1999; Godin, 2003). The basin within the Thakkhola Graben is bounded to the east and west by the Muktinath and Dangardzang Faults, respectively (figs. 4, 8, and 10). The graben-bounding faults continue as far south as the Annapurna Detachment (fig. 2) (Brown and Nazarchuk, 1993; Godin et al., 1999a; Godin, 2003), but thick accumulation of basin-fill sediment is restricted to north of the Lupra Fault (fig. 4). The northern boundary of the basin is less well defined owing to accessibility issues surrounding the Tibet-Nepal border. Analysis of SRTM elevation data coupled with Aster multi-spectral imagery has facilitated mapping of the northernmost strands of the Dangardzang Fault and the adjacent graben basin (fig 8). No obvious structure bounds the northern portion of the basin.

Figure 10a
Cross-section A-A′ is oriented perpendicular to the Thakkhola Graben and runs from the Dangardzang footwall to the Muktinath footwall. The Dangardzang Fault is modeled to be steeply dipping with two slight bends in the fault surface. These bends produce folds in the basin rocks concurrent with slip on the fault. I, II, III, and IV refer to the homoclinal dip panels found within the basin. These dip panels are separated by axial surfaces AS1, AS2, and AS3 The Muktinath Fault is interpreted to be steeply dipping without bends. AD - Annapurna Detachment, ASZ - Annapurna Shear Zone.

Figure 10b
Cross-section B-B′ is oriented parallel to the Thakkhola Graben and located within the basin. This depicts the Kagbeni Fault with an anticline in the hanging wall and a syncline in the footwall. These folds and the Kagbeni Fault are interpreted to have formed prior to graben development. AD - Annapurna Detachment, ASZ - Annapurna Shear Zone.

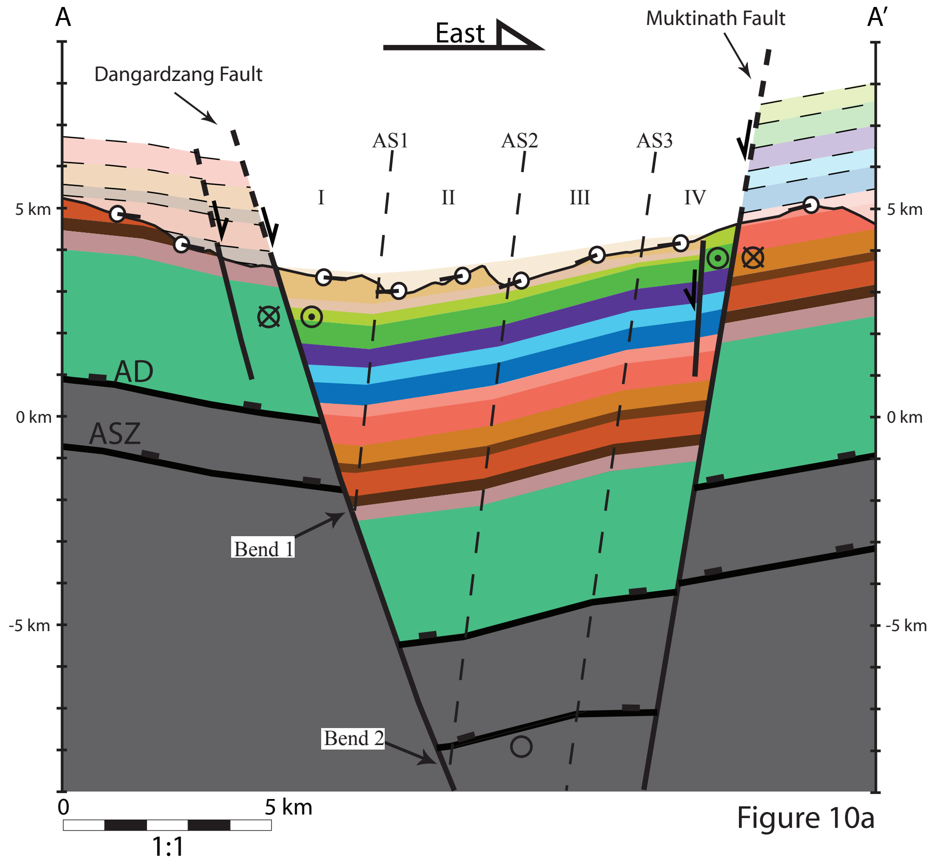

Figure 10a

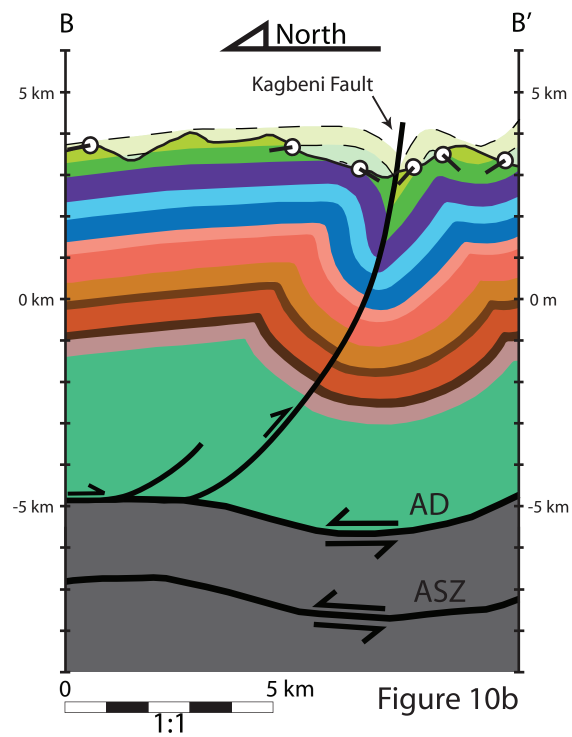

Figure 10b

The southernmost portion of the the Thakkhola Graben field map (fig. 4), up to the Kagbeni Fault, is adapted from mapping by Godin (2003). In this portion of the map east-west-trending, kilometer-scale folds in the Tethyan rocks produce topographic highs in the ridges surrounding the villages of Jomsom and Lupra (fig. 4). The rocks exposed here are, from south to north, Early Jurassic through Upper Cretaceous Tethyan Sedimentary sequence rocks with a small outcrop of the Upper Triassic *Quartzite* Formation at the intersection of the Lupra Fault with the Kali Gandaki River (fig. 4). The west-northwest-trending, steeply north dipping Lupra Fault continues until just east of the village of Lupra (fig. 4) where it is observed by Godin (2003) to be cut by a minor north-south-trending normal fault. To the north of the Lupra Fault, around Lupra Village, Godin (2003) observes the Tethyan rocks folded into an upright syncline-anticline pair, from south to north, with the *Lupra* shale exposed in the core and the *Bagung* limestone duplicated on either side (fig. 4). Moving to the north the *Lupra* shale is repeated at the base of the ridge east of Ekle Bhatti Village on the northern limb of the anticline (fig. 4). Towards the Kali Gandaki River these Tethyan rocks are covered by at least 2 generations of river terraces surrounding the villages of Lupra, Dangardzang, and Kagbeni (fig. 4). These terraces, combined with the modern fluvial deposits of the Kali Gandaki River, represent the youngest basin-fill sediments deposited within the graben. The ridges immediately south of the Kagbeni Fault are dominantly composed of the Cretaceous *Lower* and *Upper Chuck* Formations. On the ridge to the east of the Kali Gandaki River these rocks are observed to be folded into a syncline with an axial plane attitude of 097^{o}/ 80^{o} S (figs. 4, 9c, and 10b). The trace of the axial plane runs along the top of this ridge from the westernmost strand of the Muktinath Fault to the Kali Gandaki

River, however this syncline is not observable on the west side of the Kali Gandaki River (fig. 4). This suggests the presence of an undetected intervening structure near the axis of the river. The Kagbeni Fault is found within the graben at the base of the northern slopes of the ridges to the west and east of Kagbeni where it is observed to offset rocks of the Cretaceous *Chukh* Group (fig. 4). To the west of Kagbeni this fault juxtaposes *Lower Chukh* rocks in its hanging wall against *Upper Chukh* rocks in its footwall; to the east it juxtaposes two units of the *Upper Chukh* Unit, the *Dzong* Formation in the hanging wall against the *Muding* Formation in the footwall (figs. 4 and 10b). Near Muktinath Village the Kagbeni Fault is poorly exposed due to a thick accumulation of glacial sediment. One compatible fault surface was found within the Lupra shale between the villages of Jharkot and Muktinath, conservatively placing this portion of the fault between the observed traces in the basin to the west and in the Muktinath Fault footwall to the east (fig. 4). North of the Kagbeni Fault the *Chukh* rocks have been folded into a moderately south-vergent anticline with an axial plane attitude of $281^{o}/ 79^{o}$ S. We interpret to be an offset continuation of the south-vergent Thorung North anticline in the Muktinath Fault footwall and the south-vergent anticline observed north of the Kagbeni Fault in the Dangardzang Fault footwall (figs. 4, 5a, 5b, and 10b). The anticline observed in the valley represents a structurally higher and 26^{o} steeper portion of the anticline observed in the adjacent footwalls. The southern limb of this anticline dips ~ 30^{o} S (fig. 9d) towards the Kagbeni Fault and comprises the lower half of the slopes of the ridges northwest and northeast of Kagbeni (fig. 4). Small, discontinuous outcrops of *Lupra* shale are observable along the trace of the axial plane northwest of Jharkot Village where small streams have incised through the overlying *Chukh* rocks and cover deposits (fig. 4). The northern limb of the anticline is observable in the *Upper Chukh* rocks at the top of the ~ 4000 meter high ridges northwest and northeast of Kagbeni (fig. 4). This limb dips 20-40^o N towards Tetang Village where it is covered by the basin-fill *Tetang* and *Thakkhola* Formations.

North of the villages of the Chuksan and Tetang the majority of the exposed rock consists of the *Tetang* and *Thakkhola* Formations (figs. 4 and 8). These rocks have been deposited in buttress unconformity with the underlying folded TSS, angular discordance ranges from sub parallelism to nearly perpendicular. In general, the *Tetang* and *Thakkhola* Formations dip towards the Dangardzang Fault in the west (fig. 7d); the attitudes remain more or less consistent in a north-south direction but show a variation with increasing distance from the Dangardzang Fault (figs. 4, 10a). We can group the observed variation in attitudes into 4 regionally extensive dip panels consisting of, from west to east; Panel I dipping 7^o E, Panel II, dipping 11^o W, Panel III, dipping 17^o W, and Panel IV, dipping less than 4^o W (figs. 11a and 11b1-4). These dip panels are well expressed within the basin-fill sediments but within the TSS rocks they are obscured by pre-graben deformation. Therefore we have mapped the extent of the dip panels observed within the *Thakkhola* and *Tetang* Formations of figure 4. These dip panels are observable as far south as Tangbe Village and have been mapped as far north as the villages of Maran and Charang (fig. 4). They likely continue to the north but without attitudes of the basin-fill sediment for that portion of the graben it makes mapping their extent highly speculative. Panel I borders the Dangardzang Fault on the western side of the basin and extends 3-5 kilometers to the east (figs. 4 and 11a). The rocks exposed within this dip panel belong to the *Thakkhola* Formation and generally dip 7^o E away from the

Figure 11a
Map depicting homoclinal dip panels within the Thakkhola Graben basin. Panels are labeled I,II,III,IV separated by axial surfaces AS1, AS2, AS3. Panels are continuous for at least 30 kilometers along the graben. Dip of the panels is in response to changes in dip of the underlying Dangardzang Fault surface. AS1 and AS2 are active axial surfaces rooted to bends in the Dangardzang Fault surface. AS3 is a passive axial surface that moves down-dip with each increment of slip.

Basin-fill Dip Panels

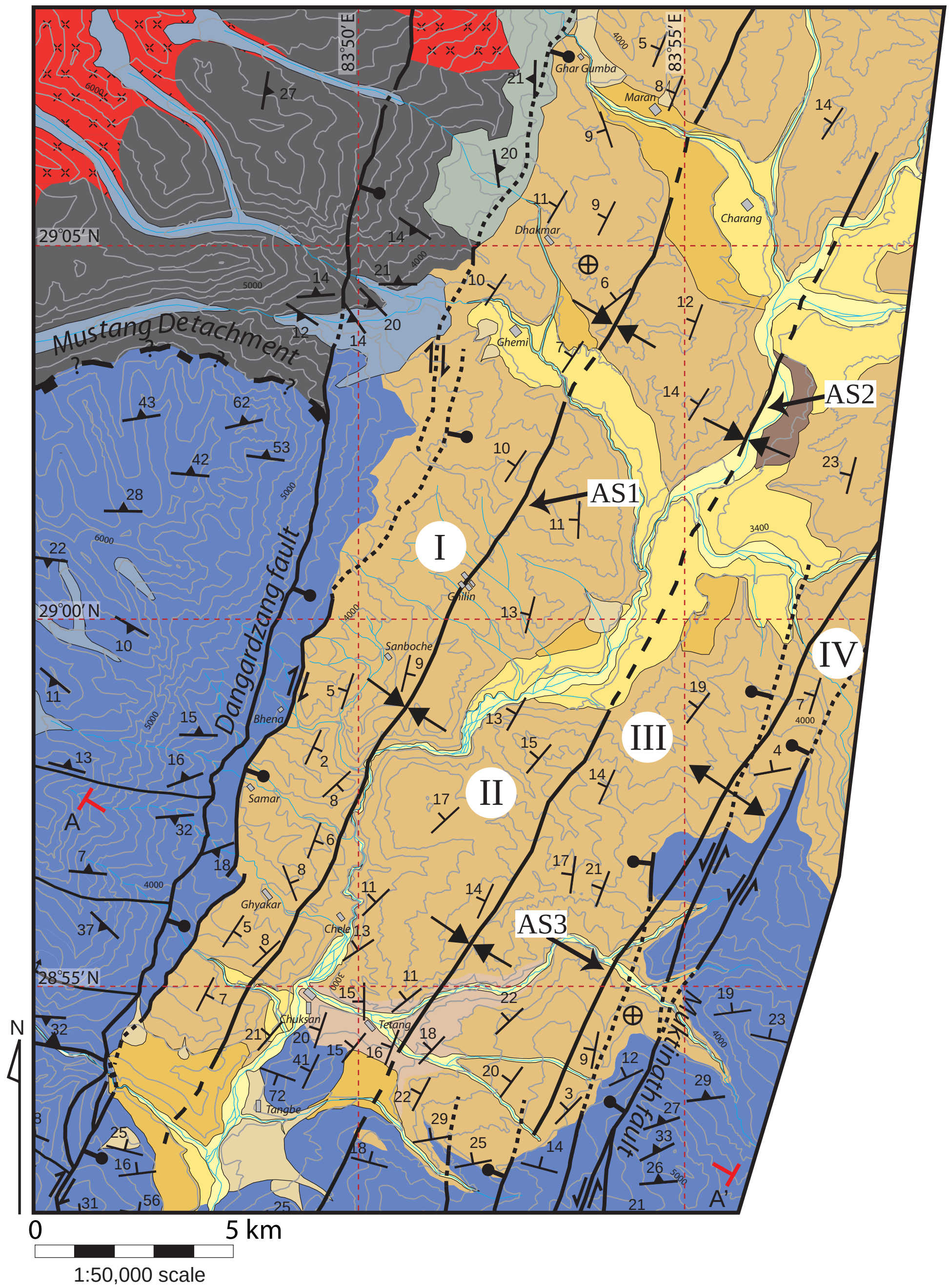

Figure 11a

Figure 11b
Stereoplots of poles to bedding planes in basin-fill dip panels. Highest concentration represents average dip panel attitude. B1 - Panel I dips 83°SE, B2 - Panel II dips 11°NW, B3 - Panel III dips 17°NW, B4 - Panel IV dips 4°NW. B5 represents the orientation of the axial surfaces separating the dip panels. AS1 - 212°/85°NW, AS2 - 221°/85°NW, AS3 - 213°/85°NW. All stereonets are equal angle, projected in the lower hemisphere.

Attitudes of Basin-fill

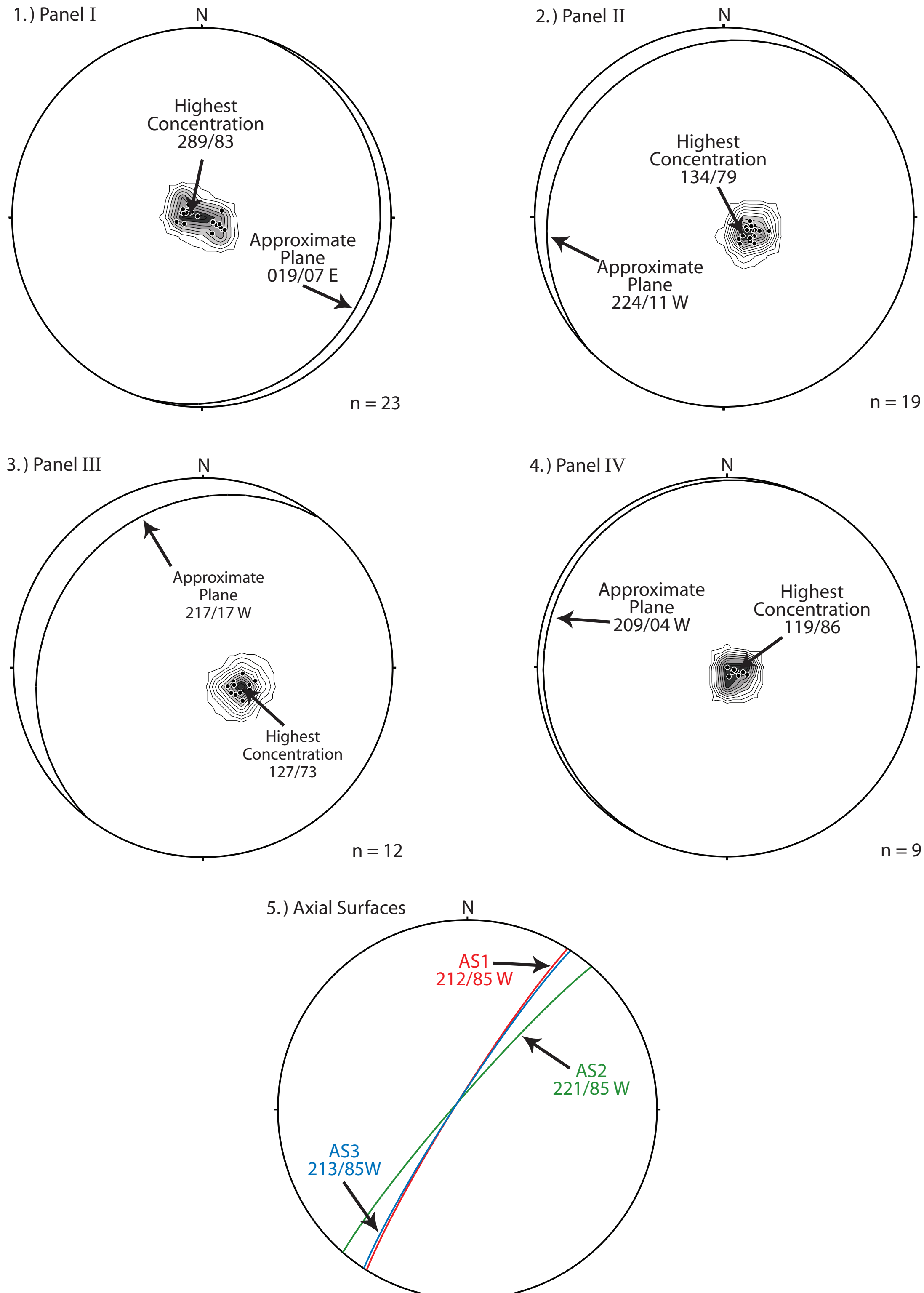

Figure 11b

Dangardzang Fault (figs. 11a and 11b1). The northern portion of Panel I dips towards the fault (fig. 4), we interpret this to be an effect of the increase in displacement observed on the western Dangardzang Fault. The shallow attitudes of the rocks in Panel I suggest primary dips except for the northern portion which appears to be rotated back towards the fault (fig. 4). Panel II is approximately 4.5 kilometers wide and is found about 5 kilometers west of the Dangardzang Fault (fig. 4 and 11a). Panel II is observable in the inclined rocks surrounding the villages of Chuksan and Tetang and is composed of the *Thakkhola* Formation and underlying *Tetang* Formation (11a). This panel dips on average 11^{o} W with dips up to 20^{o} W observed within the *Tetang* Formation (fig. 11b2). This suggests the *Tetang* has accumulated a larger magnitude of rotation and/or it was initially deposited on a steeper surface than the *Thakkhola* Formation. Panel III is about 4 kilometers wide and is observable east of Tetang Village (fig. 4 and 11a). This panel is composed dominantly of the *Thakkhola* Formation with a portion of *Tetang* Formation exposed on the western side (fig. 11a). This panel dips an average of 17^{o} W with dips observed in the *Thakkhola* Formation up to 23^{o} W (fig. 11b3). Panel IV borders the Muktinath Fault on the eastern side of the graben and is composed of rocks of the *Thakkhola* Formation (fig. 4 and 11a). This panel dips 4^{o} W with some attitudes as low as 0^{o} (fig. 11b4). These 4 regionally extensive dip panels are separated by 3 axial surfaces labeled, from west to east; AS1, AS2, and AS3 (figs. 10a and 11a). The trend of these axial surfaces parallel the Dangardzang Fault and are continuous for at least 50 kilometers (figs. 4 and 11a). The strike of these axial surfaces is determined by bisecting the average strikes of adjacent dip panels. AS1 separates Panel I and Panel II and strikes 212^{o} (fig. 11b5). AS2 separates Panel II and Panel III and strikes 221^{o} (fig. 11b5). AS3 separates Panel III and Panel IV and strikes 213^{o} (fig. 11b5). The dip of the axial surfaces is very steep, around 85^{o} W.

Basin-fill Fold Interpretation

Based on (1) the trend of the dip panels paralleling the Dangardzang Fault and (2) the large scale of these dip panels suggesting a deeply rooted cause; we have interpreted the variation in panel attitudes to be attributed to inclined shear imposed on the hanging wall as it moves over slight bends in the Dangardzang Fault surface (fig. 10a). According to Xiao and Suppe (1992) moving over a bend that results in a shallower fault dip will cause the dip of the hanging wall to increase towards the fault and vice versa. Adjacent dip panels will be separated by an axial surface that roots into a fault bend at an angle parallel to the angle of inclined shear. A dip angle of 85^{o} W has been determined through observation of steeply dipping small displacement shear fractures within the basin-fill, therefore these axial surfaces strike 212-221^{o} and dip 85^{o} W (fig. 11b5). The increase in dip from Panel I to Panel II and from Panel II to Panel III is interpreted to be the result of a slight decrease in the dip of the Dangardzang Fault occurring where AS1 and AS2 root into the fault surface (fig. 10a). AS1 and AS2 are active axial surfaces, separating rocks that have not yet passed over their respective bends from those that have, as such they are tied to the bends in the fault surface and do not move with displacement. The horizontal Panel IV represents rocks that have never passed over a bend in the fault. These rocks were originally down-dip of the bend at AS2 and have only passed over a fault surface with constant dip so they retain their original orientation. AS3 is therefore interpreted to be a passive axial surface that initiated at AS2 and moved with the hanging wall with each increment of slip. The passive axial surface associated with AS1 has been translated through the bend at AS2 and it is no longer observable.

Fractures

A total of 239 fractures measurements were collected; 128 from the footwalls of the Muktinath and Dangardzang Faults and 111 within the basin. The majority of the fractures measured were mode-1 (161 fractures) with the rest being mode-2 (68 fractures). On the basis of position and style the fractures were divided into 4 groups; A - Footwall Mode-1, B - Footwall Mode-2, C - Basin Mode-1, and D - Basin Mode-2 (fig. 12a-d). These groups were analyzed by plotting poles to fracture planes and contouring the data to highlight concentrations. Planes are then constructed to represent the orientation of concentrations. We collected 104 footwall mode-1 fractures these are typically closed but contain calcite fill when open. Two sets of mode-1 fractures occur in the footwall rocks; set 1 oriented at 014^o/83^o E and set 2 oriented at 106^o/73^o S (fig. 12a). Set 1 cross-cuts set 2 and is the highest concentration of fractures. The orientation of Set 1 is sub-parallel to the Dangardzang and Muktinath Faults while set 2 is almost orthogonal to them. There was a minor amount of mode-2 fractures observed in the footwalls (14). These typically have very little offset with some up to a few centimeters. Three sets of mode-2 fractures are observed in the footwall rocks; set 1 oriented at 143^o/90^o, set 2 oriented at 223^o/48^o W, and set 2' oriented at 031^o/79^o E (fig. 12b). Set 1 contains the highest concentration and set 2 and 2' contain sub-equal concentrations. No clear cross-cutting relationship between these sets was observed in the field. Within the basin 57 mode-1 and 54 mode-2 fracture measurements were collected. These measurements were mostly collected within the *Thakkhola* and *Tetang* Formations.

Figure 12
Stereoplots representing the orientation of fractures by location and style of fracture. Sets of fractures are labeled with 1 being the highest concentration. In the case of two equally concentrated sets they will be labeled using the same number one of which will be modified with an apostrophe (e.g. 1 and 1'). A - set 1 oriented parallel to the graben is interpreted to be linked to east-west extension and activity on the Dangardzang and Muktinath Faults, set 2 oriented orthogonal to the graben is interpreted to be an older set related to the folds observed in the Tethyan rocks. B - these shear fractures are interpreted to be Riedel shears related to strike-slip movement on the Dangardzang and Muktinath Faults. C, D - the basin fractures are interpreted to be related to inclined shear imposed on the hanging wall as it moves along the Dangardzang Fault. They are oriented roughly parallel to the orientation of the basin axial surfaces.

Figure 12 Fracture Stereoplots

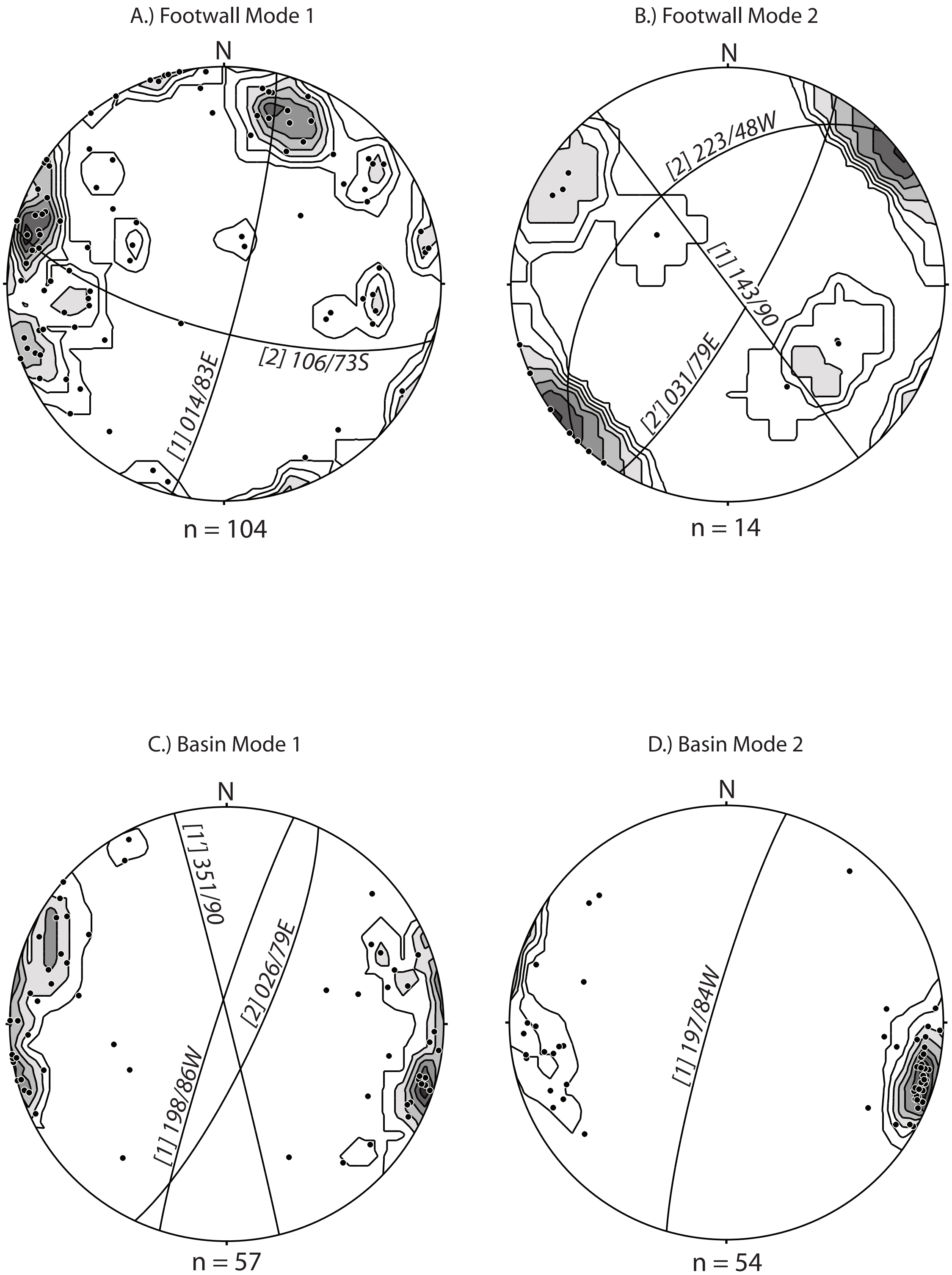

Mode-1 fractures within the basin are unfilled. Three concentrations have been observed; set 1 oriented at $198^o/86^o$ W, set 1’ oriented at $351^o/90^o$, set 2 oriented at $026^o/79^o$ E (figs. 12c and 13a). Set 1 and 1’ are the dominant orientations of mode-1 basin fractures, set 2 is a minor set. Sets 1 and 2 are sub-parallel to the Dangardzang and Muktinath Faults and set 1’ is approximately 30^o oblique to them. The shallower fractures of set 2 cross-cut the fractures of sets 1 and 1’. These later stage set 2 fractures may be associated with east-dipping meter-scale intra-formational faults observed to cross-cut fractures in the basin-fill (fig. 13a). Mode-2 fractures within the basin typically have offsets on the order of a few centimeters with some having coalesced into steeply west-dipping intra-formational faults with offsets of a few meters (fig. 13b). Shear along these fractures is down towards the Dangardzang Fault. One set of mode-2 fractures has been observed oriented at $197^o/84^o$ W (figs. 12d and 13a). This set is parallel to the orientation of the Dangardzang and Muktinath Faults.

Fracture Interpretation

In general the fractures observed in the basin and in the adjacent footwalls show two dominant orientations. Fractures oriented parallel to the basin-bounding faults were the most common and these were observed in the basin-fill formations as well as the Tethyan rocks. The second, less common trend was in fractures oriented roughly orthogonal to the basin-bounding faults. Fractures of this basin-orthogonal trend were only found within Tethyan rocks and they are cross-cut by fractures of the basin-parallel trend. This suggests that two generations of fractures are represented in the basin and surrounding footwalls; an earlier set of fractures striking approximately east-west and a later set of fractures striking approximately north-south. The earlier set of fractures cross-

Figure 13
Images showing fractures within the basin-fill units.
A - closely spaced nearly vertical mode-1 and mode-2 fractures within thin-medium bedded sandstones and conglomerates. Moderately dipping normal faults occasionally cross-cut the fractures. B - widely spaced steeply dipping mode-2 fractures within thick bedded sandstones and conglomerates. Reference horizon is denoted with a blue dashed line.

Figure 13

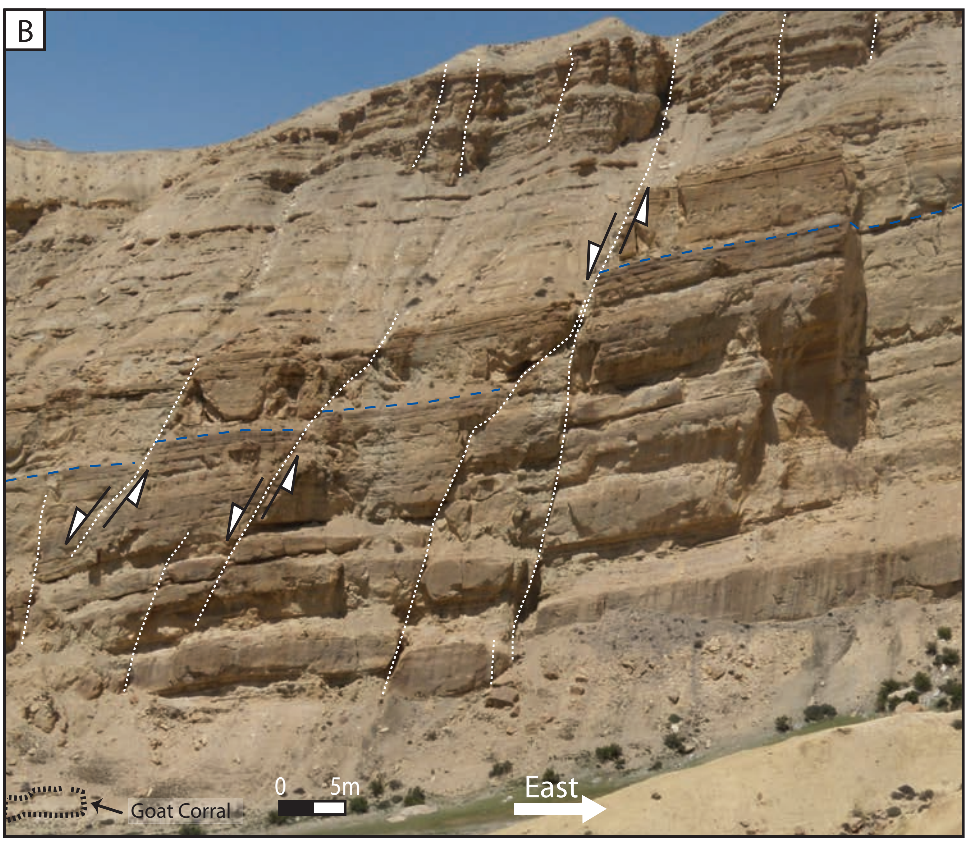

cuts folds associated with pre-graben deformation of the Tethyan rocks. This set can be correlated with the D_4 phase of deformation of Godin (2003). The later set of fractures is most likely associated with development of the Thakkhola Graben and can be correlated with the D_5 deformation phase of Godin (2003). We have interpreted the mode-2 fractures of D_5 to be the product of inclined shear imparted to the hanging wall as it moves over bends in the Dangardzang Fault. These have been used to ascertain the dip angle of the axial surfaces emanating from bends in the fault surface. Modeling hanging wall deformation through inclined shear has been accomplished through Midland Valley's 2DMove forward kinematic modeling software. The geometry of the deformed hanging wall and attitude of basin parallel fractures were used as inputs to constrain the geometry of the Dangardzang Fault surface.

Muktinath Fault

The Muktinath Fault bounds the eastern side of the Thakkhola Graben and is composed of a series of sub-parallel faults that have been mapped as far south as the Annapurna Range and into southern Tibet where their termination is not clearly defined (Bordet et al., 1971; Colchen et al., 1981) (fig. 2). We have mapped this set of faults for approximately 30 kilometers from the western slopes of Thorung South to the mountains east of Tetang Village (figs. 4 and 14a). In the southwestern portion of the mapping area the faults cut through Jurassic Tethyan carbonate rocks. Activity on the Muktinath Fault has facilitated exhumation of the peaks of Thorung North and South (fig. 15a). Figure 15a shows a view of Thorung North where the two easternmost strands of the Muktinath Fault have offset the overturned limb of the Thorung North anticline. The horst block, dipping 45^{o} N, is a structurally higher portion of the fold seen in the background footwall,

Figure 14

A - Google Earth image looking east towards Thorung La Valley. The Kagbeni Fault is shown offset along two strands of the Muktinath Fault. Locations of Muktinath Fault striae measurements are shown. A1 - depicts purely dip-slip motion. A2 - depicts two sets of striae, the set in red is oblique with dominantly strike-slip and the set in blue is oblique with dominantly dip-slip. The red set occurred first according to overprinting relationships observed in the field. A3 - depicts purely dip-slip motion on two fault surfaces. The Kagbeni Fault is offset with an apparent left-lateral sense.

B - stereoplot representing all Muktinath Fault slip lineations. The highest concentration (set 1) is oblique with dominantly strike-slip motion, the lower concentration (set 2) is almost pure dip-slip.

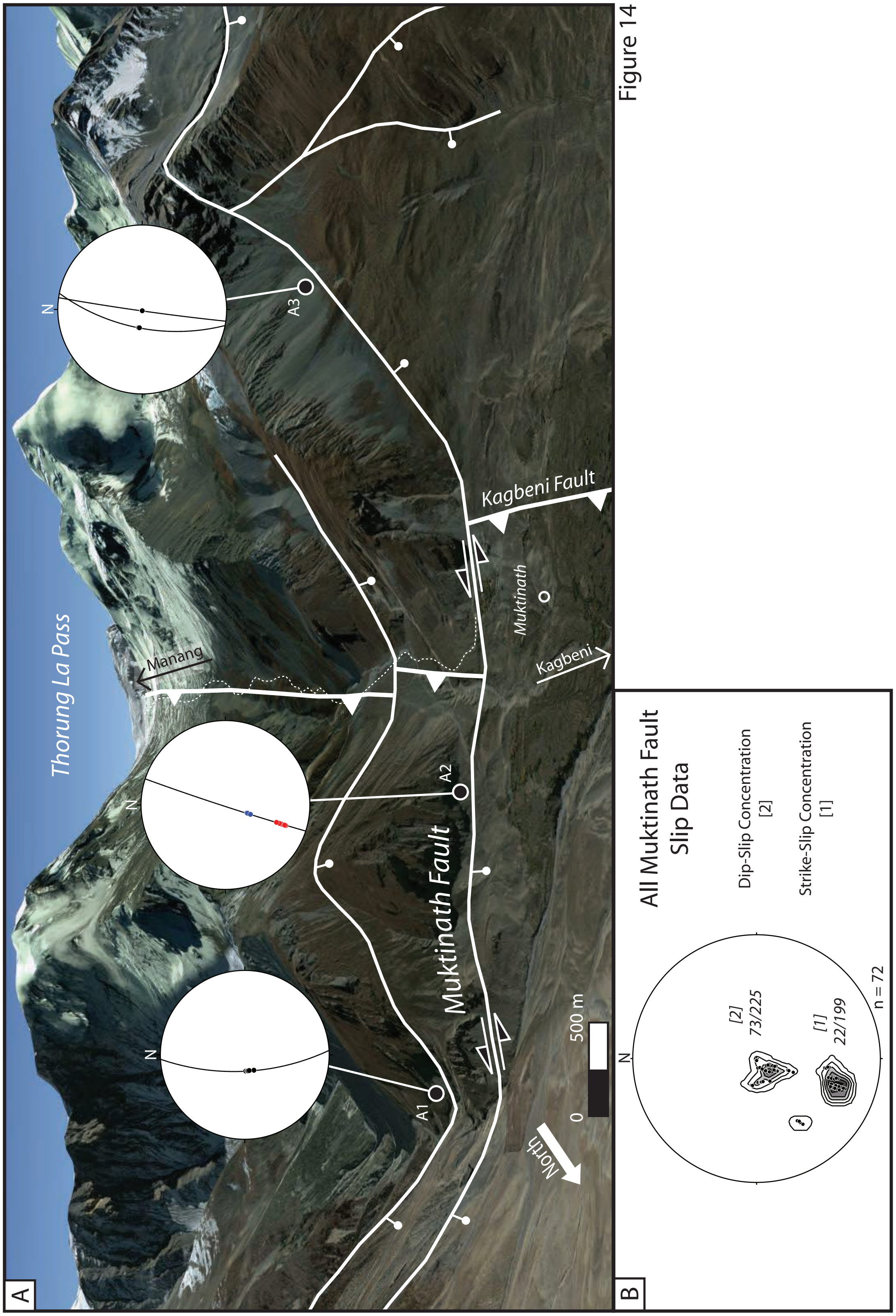
A
Thorung La Pass
Manang
Kagbeni Fault
Muktinath
Kagbeni
Muktinath Fault
A1
A2
A3
N
0
500 m
North
B
All Muktinath Fault
Slip Data
Dip-Slip Concentration
[2]
Strike-Slip Concentration
[1]
[2]
73/225
[1]
22/199
n = 72

Figure 14

dipping 80^{o} N. The portion of the fold within the horst block is even more overturned than the portion in the footwall. These two strands of the Muktinath Fault converge and share a common trace for a few kilometers before diverging again. There is no clear cross-cutting relationship between these two fault traces (fig. 4). Two shorter faults (5-10 km-long) have been found north of Muktinath Village, these cut through Cretaceous Tethyan rocks. The westernmost fault, running between Jharkot and Muktinath Villages, is continuous for approximately 10-15 kilometers in our mapping area and has been observed to the south for some 10's of kilometers (Godin, 2003). The Muktinath Fault is difficult to track in the north due to thick accumulations of basin-fill sediment and accessibility issues around the Tibet-Nepal border (fig. 15b).

These fault traces display two common orientations: one set is oriented approximately 000^{o}-010^{o}; the other set oriented approximately 030^{o}-045^{o}, from south to north (fig. 4). The transition between these two sets is gradual and occurs east of Tangbe Village. The faults making up the eastern boundary of the Thakkhola Graben dip steeply to the west at 80-90^{o} and are interpreted to cut down to at least 5 kilometers below sea level (fig. 10a). Two sub-equal concentrations of fault striae have been found on these faults: set 1 oriented at 22^{o}/199^{o}; set 2 at 73^{o}/225^{o} (fig. 15b). Set 1 is oblique with a dominantly sinistral strike-slip component and set 2 is almost pure dip-slip. A clear overprinting relationship for these striae has been observed on the northern wall of Thorung La pass (fig. 15a). Stereoplot A2 shows a set of strike-slip-oblique striae (in red) overprinted by a set of dip-slip striae (in blue), implying strike-slip-oblique movement followed by dip-slip movement. The easternmost faults appear to have accommodated the highest magnitude of strain with a stratigraphic separation of approximately 3.5

Figure 15
A - photomosaic of the Thorung North peak viewed from the north. The Muktinath Fault offsets the Thorung North anticline and lowers a structurally higher portion of the fold. Overturned subvertical beds in the background are from the lower limb of the anticline. The overturned moderately dipping beds in the horst block are from a portion of the anticline that is closer to the hinge.
B - Image from the Thakkhola Graben basin showing nearly horizontal basin-fill strata resting in buttress unconformity to the folded Tethyan rocks below. The basin-fill has buried a portion of the Muktinath Fault. The Cretaceous-Jurassic contact is offset across the western Muktinath Fault strand.

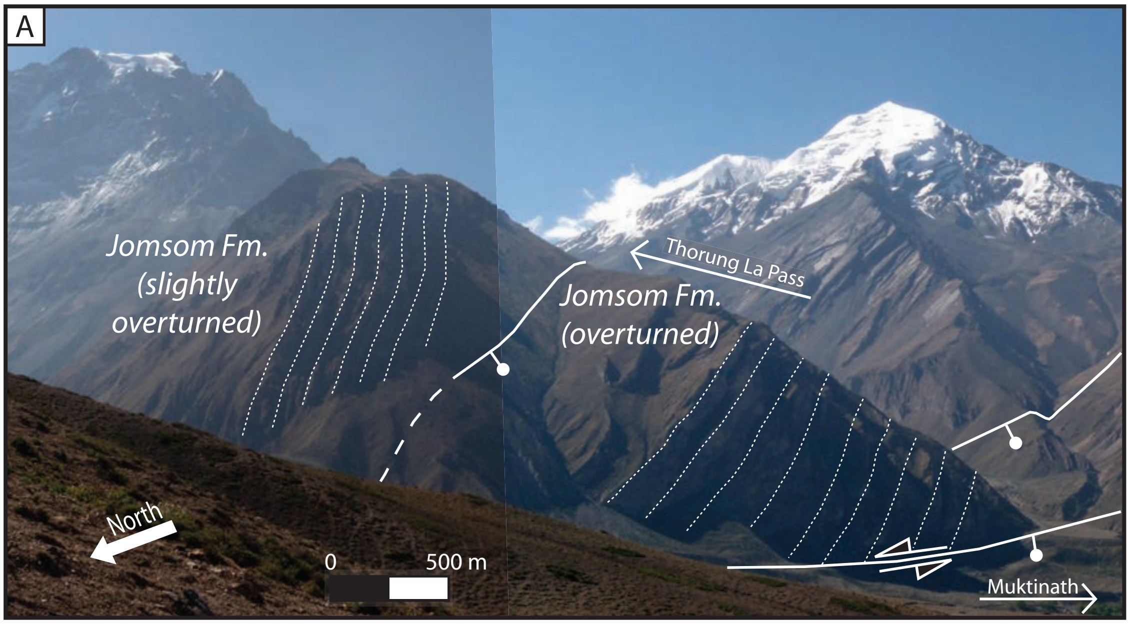
A
Jomsom Fm.
(slightly
overturned)
Jomsom Fm.
(overturned)
Thorung La Pass
North
0
500 m
Muktinath

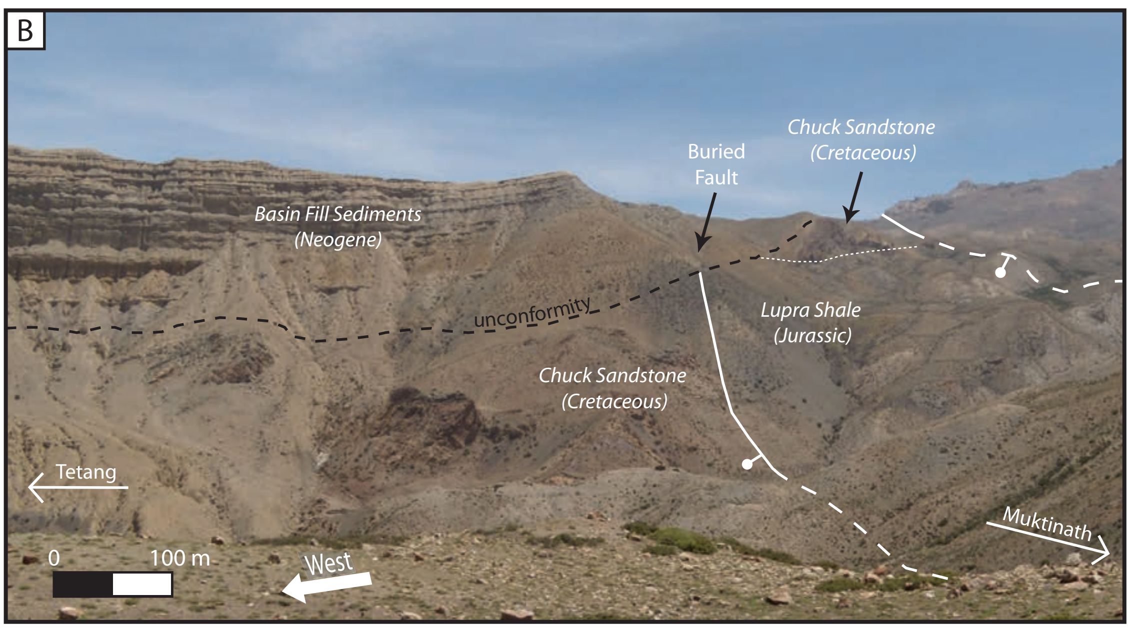
B
Chuck Sandstone
(Cretaceous)
Buried
Fault
Basin Fill Sediments
(Neogene)
unconformity
Lupra Shale
(Jurassic)
Chuck Sandstone
(Cretaceous)
Tetang
0
100 m
West
Muktinath

Figure 15

kilometers (fig. 10a). The westernmost fault expresses approximately 1 kilometer of stratigraphic separation (fig. 4). The shorter length faults have separations of less than 1 kilometer. The eastern boundary of the Thakkhola Graben appears to have formed in two phases; sinistral strike-slip faulting followed by normal faulting. Cross-cutting relationships are unclear but faulting appears to step basin-ward and towards the south with time. The long, relatively high magnitude eastern and western faults might have formed as *en echelon* faults with the shorter faults accommodating strain within the intervening relay (fig. 4).

Dangardzang Fault

The Dangardzang Fault bounds the western side of the Thakkhola Graben from the Dhaulagiri Range in the south to the Indus Yalu Suture in the north (Bordet et al., 1971; Colchen et al., 1981) (fig. 2). We have mapped the Dangardzang Fault north of Kagbeni Village for approximately 100 kilometers. Figure 4 depicts 40 kilometers of the Dangardzang Fault based on field mapping; the Jomsom-Kagbeni area included from Godin (2003), Kagbeni Village and north from this work. Figure 8 shows the continuation of the Dangardzang Fault as inferred by remote-sensing based mapping. The Dangardzang Fault consists of two parallel faults over the majority of its length. In the south the faults are separated by only a few hundred meters with both strands expressing a few thousand meters of stratigraphic separation (fig. 4). West of Kagbeni Village the fault strands merge for approximately 2 kilometers until the valley leading to Santha Village where the western strand appears again (fig. 15a). Stratigraphic separation is very low (around 200 meters) for this portion of the western fault. Moving northward the fault strands diverge to approximately 2.5-3 kilometers and separation on the western fault

Figure 16

A - Google Earth image of the Dangardzang Fault near the village of Kagbeni looking west. The Kagbeni Fault is shown offset along the Dangardzang Fault. Locations of Dangardzang Fault striae measurements are shown. A1 - depicts a mixture of purely dip-slip and oblique-slip motion. A2 - depicts oblique but dominantly dip-slip motion on a range of fault surfaces. One surface shows two sets of striae, the red set is oblique with dominantly strike-slip motion and the blue set is dominantly dip-slip. The red set is interpreted to have been formed first according to field observations. The Kagbeni Fault is offset with an apparent right-lateral sense. B - stereoplot representing all Dangardzang Fault slip lineations. The highest concentrations (sets 1 and 1') are almost purely dip-slip, the lowest concentration (set 2) is strike-slip.

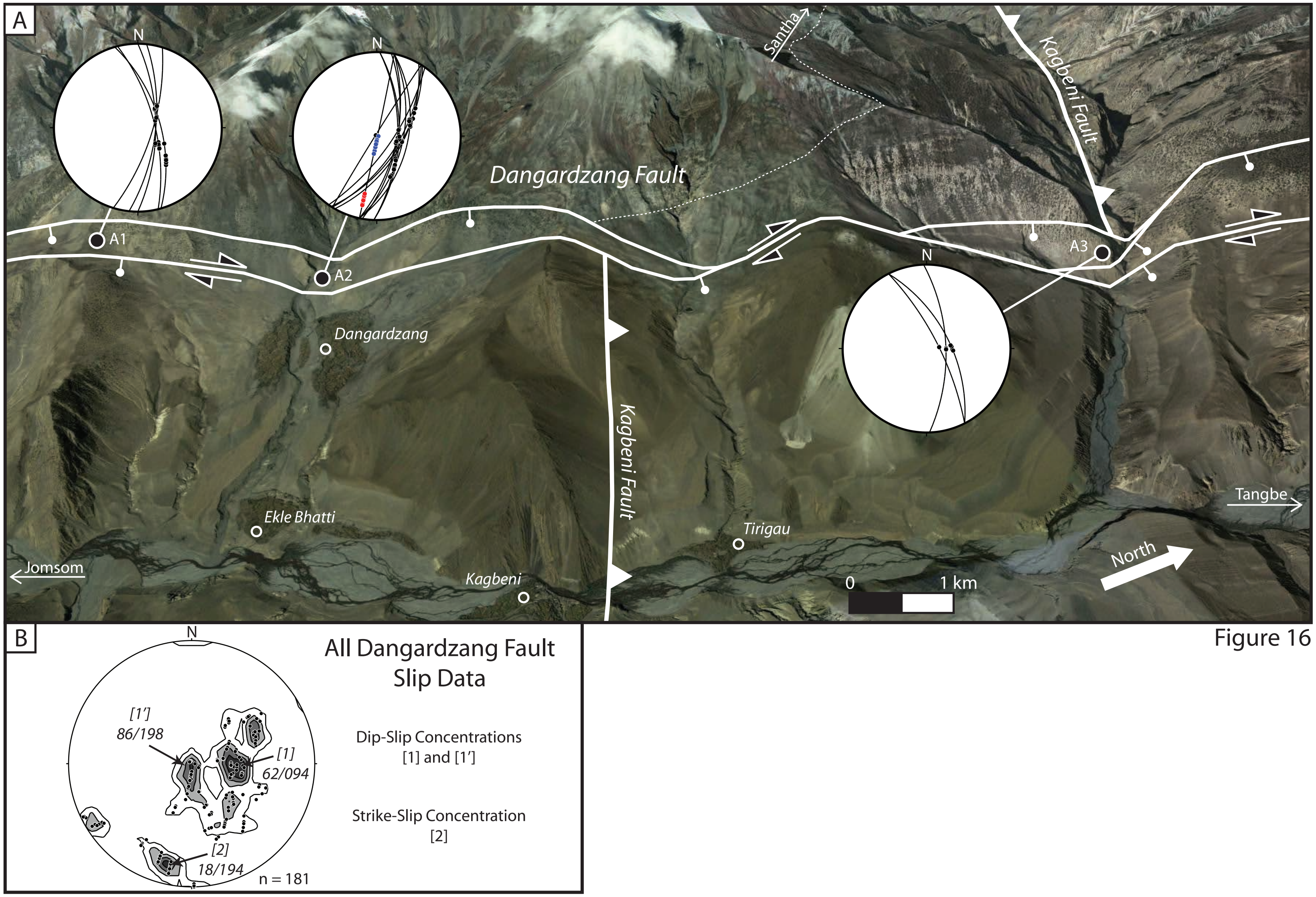
A
N
A1
A2
A3
Dangardzang Fault
Kagbeni Fault
Kagbeni Fault
Santha
Dangardzang
Ekle Bhatti
Kagbeni
Tirigau
Jomsom
Tangbe
North
0
1 km
B
All Dangardzang Fault
Slip Data
[1′]
86/198
[1]
62/094
[2]
18/194
n = 181
Dip-Slip Concentrations
[1] and [1′]
Strike-Slip Concentration
[2]

Figure 16

increases to about 1 kilometer (fig. 4). The eastern fault is buried for the northern half of its extent where basin-fill sediment is juxtaposed against the Dolpo-Mugu and Mustang granites (fig. 8). Within southern Tibet the easternmost Dangardzang Fault is expressed through dextral offset of several ridges and streams immediately adjacent to the basin. The westernmost fault is observable as a linear arrangement of small fault scarps. These strands are separated by 6-8 kilometers. The northern termination of the Dangardzang Fault is unclear but the fault strands can be tracked at least as far as 29°45'N.

A bend in the trace of the Dangardzang Fault appears near the Tibet-Nepal border (fig. 8). South of the border the fault trace is oriented between 025° and 035°; north of the border it is oriented 000° to 010°. In cross-sectional view there are two slight bends in the surface of the easternmost Dangardzang Fault, Bend 1 at 2 kilometers below sea level and Bend 2 at 8 kilometers below sea level (fig. 10a). At the surface the fault dips 74° E, then 70° E below Bend 1, and 67° E below Bend 2. The Dangardzang Fault is interpreted to cut down to at least 10 kilometers below sea level (fig. 10a). This fault geometry was modeled in order to be consistent with the observed basin-fill deformation using Midland Valley's 2DMove forward modeler. Three concentrations of fault striae have been measured for the Dangardzang Fault: set 1 oriented at 62°/094°; set 1' at 86°/198°; and set 2 at 18°/194 (fig. 15b). Set 1 and 1' were equally abundant and both indicative of dip-slip motion. Set 2 was less abundant than 1 and 1' and was indicative of dominantly dextral strike-slip-oblique motion. Several fault surfaces show dip-slip striae (in blue) overprinting strike-slip striae (in red) as is depicted in stereoplot A2 (fig. 15a). This implies the western boundary of the Thakkhola Graben initiated as a dextral strike-slip-oblique fault and evolved into a dip-slip fault. No clear cross-cutting relationship exists between the western and eastern fault strands but the relationship of dip-slip overprinting strike-slip implies the western fault, which expresses only dip-slip motion, may have formed after the initial dextral strike-slip on the graben-bounding fault.

Kagbeni Fault

The Kagbeni Fault extends across the width of the mapping area and consists of three offset fault segments correlated on the basis of geometry, kinematics, and structural position. The Kagbeni Fault is observable in the Dangardzang Fault footwall near the village of Santha (fig. 17a), in the Muktinath Fault footwall along Thorung La Valley, and within the graben basin near the villages of Muktinath and Kagbeni (fig. 4). This fault was initially described by Godin (2003) as part of the Kagbeni structure in cross-section F-F'. Field mapping shows 5-6 kilometers of separation with an apparent right-lateral sense between the western and central segments along the Dangardzang Fault (fig. 4). The central and eastern segments are separated 1 kilometer with an apparent left-lateral sense along the Muktinath Fault (fig. 4). There is very little separation observed along the subsidiary Muktinath faults found within the basin. The three fault segments dip 60^{o} N at the surface and exhibit approximately east-west strikes. Within the Muktinath footwall the Kagbeni Fault cuts through the core of an isoclinal syncline between the Thorung North and South anticlines (cross-section D-D' of fig. 5b). Within the basin (cross-section B-B' of fig. 10b) and in the Dangardzang footwall (cross-section C-C' of fig. 5a) the Kagbeni Fault cuts through a syncline between two anticlines. In all three locations the Kagbeni Fault contains a south-verging anticline in its hanging wall and an upright to north-verging anticline in its footwall. The Kagbeni Fault is interpreted to become shallower at depth until it soles into the upper Annapurna Detachment (figs.

Figure 17
A - image of Kagbeni Fault in the hanging wall of Dangardzang Fault near Santha Village. Bedding planes are highlighted with white dotted lines. The Kagbeni Fault cuts and offsets a syncline in the Tethyan rocks. Units in the footwall and hanging wall dip towards the fault. B - stereoplot of all striated fault planes for the Kagbeni fault and their concentrations. Two concentrations of fault slip lineations are identified (set 1 and 2) and both are purely dip-slip. All stereoplots are equal angle and projected in the lower hemisphere.

Figure 17

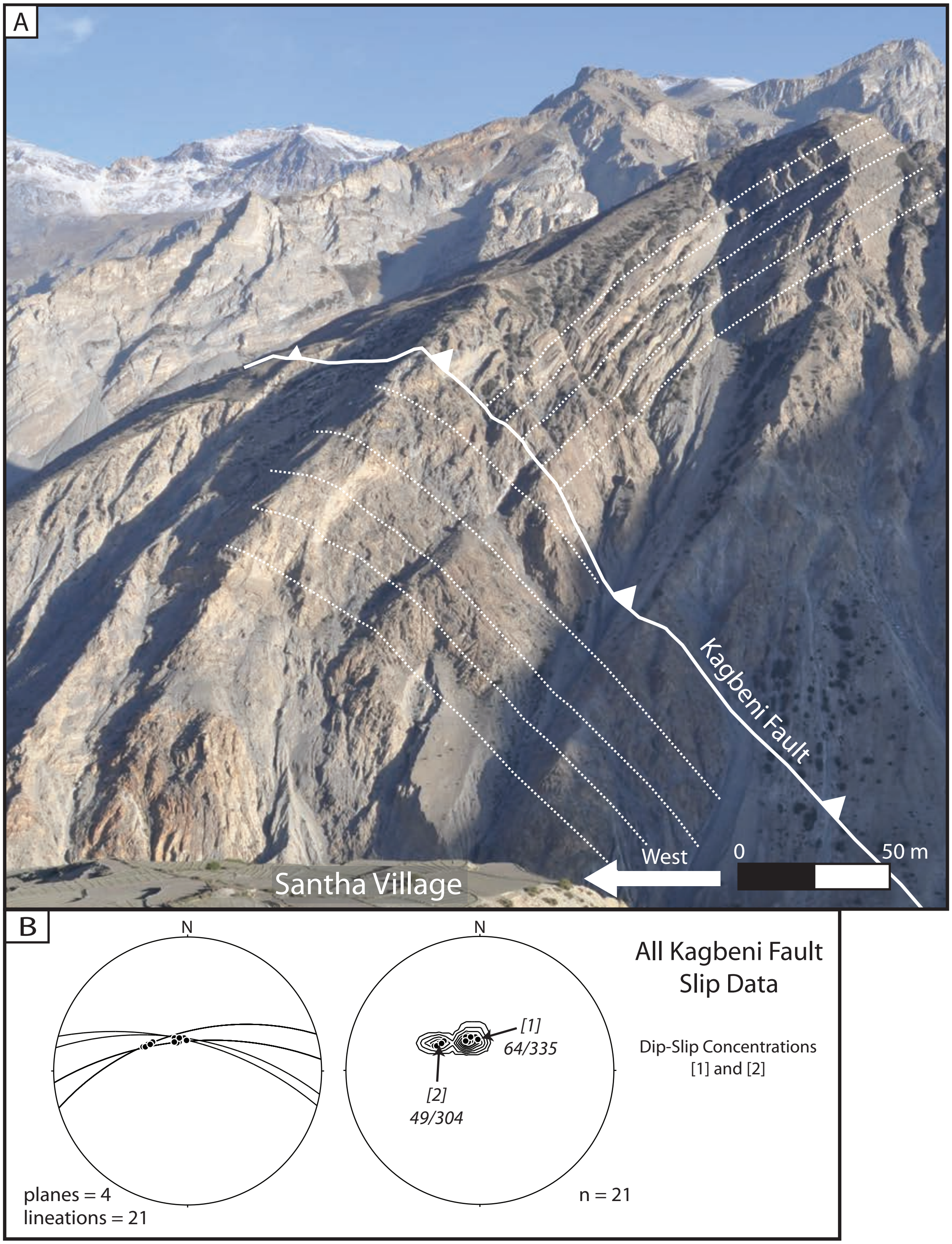
A
Kagbeni Fault
West
0
50 m
Santha Village
B
N
planes = 4
lineations = 21
N
[1]
64/335
[2]
49/304
n = 21
All Kagbeni Fault
Slip Data
Dip-Slip Concentrations
[1] and [2]

5a,b and 10b). Few fault surfaces are available for observation due to inaccessibility and erosion. Four surfaces were found with strikes ranging from 254^{o}-285^{o} and dips ranging from 58^{o}-65^{o} N (fig. 17b). There are two concentrations of dip-slip striations on the fault surfaces: set 1 is oriented $64^{o}/335^{o}$ and set 2 is oriented $49^{o}/304^{o}$. This kinematic data for the Kagbeni Fault is compatible with the D_4 south-verging compressional phase of deformation for the Tethyan rocks (Godin, 2003).

Lupra Fault

The Lupra Fault was originally recognized by Colchen et al. (1986) and was subsequently mapped by Godin (2003). This fault strikes approximately 290^{o} and dips 60^{o}-70^{o} N (Godin, 2003 and this work fig. 5a). The Lupra Fault is found in the Dangardzang footwall and in the western half of the basin south of the village of Lupra, no evidence for it is found in the Muktinath footwall. It has been suggested that the Lupra Fault initiated as a reverse-sense fault prior to the development of the Thakkhola Graben and then was reactivated as a normal-sense fault during the graben's evolution (Godin, 2003). Field mapping reveals no offset of the Lupra Fault along any graben-bounding faults (fig. 4), precluding the possibility of its operation before the development of the Dangardzang Fault. Instead we propose the Lupra Fault initiated during as a final stage in graben development once the Dangardzang footwall and hanging wall began to recouple. We have interpreted the Lupra Fault to shallow at depth where it soles into the upper Annapurna Detachment (fig. 5a). No fault surfaces were observed for the Lupra Fault.

Mustang Detachment

Field work in the Dangardzang footwall to the west of the village of Ghemi reveals a previously unrecognized structural and metamorphic discontinuity herein referred to as the Mustang Detachment (fig. 4). Accessibility is restricted by extreme terrain and proximity to the Nepal-Tibet border and as such no direct observation of the detachment was possible. The Mustang Detachment is a boundary between unmetamorphosed Tethyan rocks in the hanging wall and metamorphosed lowermost Tethyan rocks or Greater Himalayan rocks in the footwall. The immediate hanging wall rocks are the Carboniferous through Triassic marine sedimentary rocks of the TSS. These rocks have experienced low-grade diagenetic alteration and lack ductile shear fabrics. No recystallized sandstones or phyllitic shales are observed above the detachment. In the immediate footwall of the Mustang Detachment there is a sharp increase in metamorphic grade. These rocks consist of quartzites, phyllites, marbles, garnet-staurolite schists, and calc-silicate gneisses. We have interpreted these lithologies to be consistent with either the lowermost Tethyan rocks or more likely the uppermost Greater Himalayan rocks. The footwall rocks have been pervasively intruded by leucogranite pods, sills, and dikes. These leucogranites cross-cut the dominant foliation and are themselves sheared, implying that these intruded contemporaneously with the country rock deformation. These leucogranite bodies most likely emanate from the Dolpo-Mugu and Mustang Leucogranites (fig. 4). No leucogranite bodies are observed in the hanging wall of the Mustang Detachment. The Mustang Detachment also represents a structural discontinuity between the macroscopically folded Tethyan rocks above and the nearly homoclinal foliation found in the metamorphic rocks below (fig. 6). More work remains to be done to ascertain the viability and position of this detachment, however our observations suggest a comparison to the Phu Detachment in the Manaslu region east of the Thakkhola Graben (Searle and Godin, 2003) (fig. 2). Both of these detachments act as similar structural and lithological boundaries, leading us to assert that the Mustang Detachment is the brittle contact commonly referred to as the upper Annapurna Detachment (Brown and Nazarchuk, 1993; Godin et al., 1999a; Godin, 2003). This also implies the Dolpo-Mugu and Mustang Leucogranites belong to the Higher Himalayan Granite Belt which is restricted to the footwall of the South Tibetan Detachment System as opposed to the North Himalayan Granite Belt which is reported to intrude into the Tethyan rocks in the footwall of the STD.

Strain Magnitude Evaluation

The magnitude of strain accommodated by the Dangardzang and Muktinath Faults has been evaluated through the identification and geometrical analysis of common piercing points found on adjacent sides of the graben-bounding faults. The intersection of the *Bagung-Jomsom* lithological contact with the surface of the Kagbeni Fault defines a suitable piercing line that can be located in the hanging wall and both footwalls of the Thakkhola Graben (figs. 5a,b and 10b) Block models were made by aligning the long axis of a rectangular prism with the strike direction for the Muktinath Fault and Dangardzang Fault (figs. 18 and 19, respectively). The geometry of the Kagbeni Fault as well the position of the *Bagung-Jomsom* contact on the hanging wall side of the Kagbeni Fault are projected into the block model, positioned to represent their respective three dimensional orientation in the hanging wall and footwall of the basin-bounding fault to be analyzed. Scales are represented on the edges of the block diagram in order for relative

Figure 18
Model for reconstructing piercing points along the Muktinath Fault. A - block diagram showing geometrical relationship with the offset Kagbeni fault along the Muktinath Fault. Gray plane represents the Muktinath Fault which dips 81°W. The position of the Kagbeni Fault in the hanging wall of the Muktinath Fault is represented in red. The position of the Kagbeni Fault in the footwall of the Muktinath Fault is represented in dark blue. Light blue represents the position of the piercing line defined by the intersection of the *Bagung-Jomsom* contact with the Kagbeni Fault. The red and dark blue circles represent the piercing point defined by the intersection of this piercing line with the Muktinath Fault surface. The red circle represents the hanging wall piercing point and the dark blue circle represents the footwall piercing point. The positions of these piercing points are projected onto axes representing increments of dip-slip, strike-slip, and extension. The magnitude of dip-slip is 4.2 km, strike-slip is 1.9 km, and extension 0.8 km. B - diagram representing the plane containing the slip vector with respect to north. The slip vector plunges 65°, trends S38° W, and has a magnitude of 4.7 km.

A. Muktinath Fault

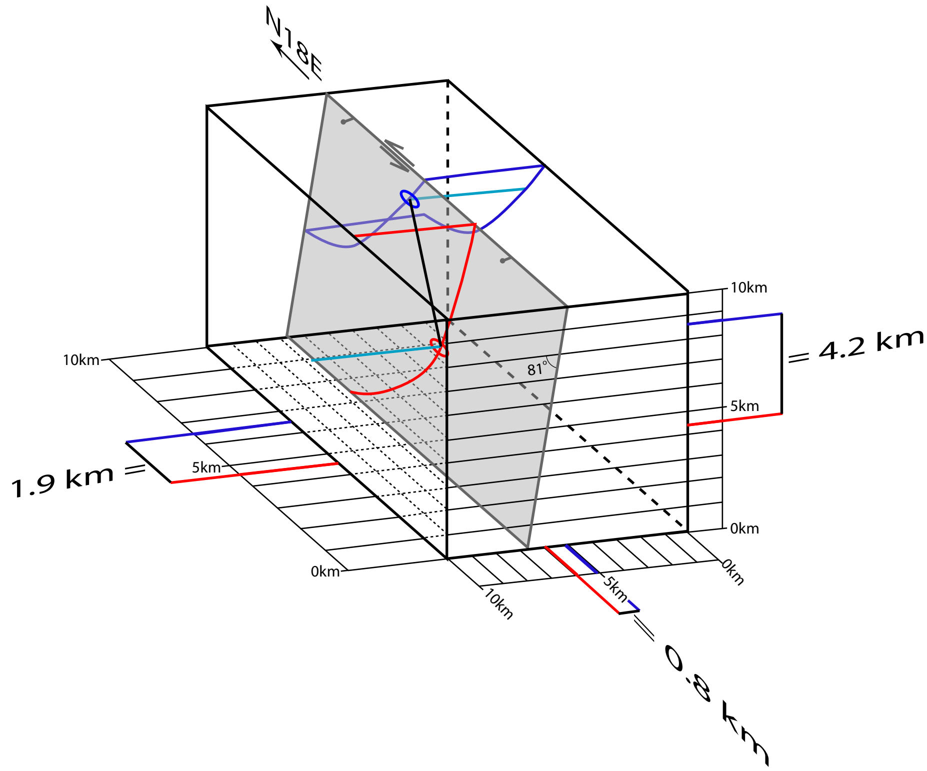

B. Muktinath Fault
Slip Vector

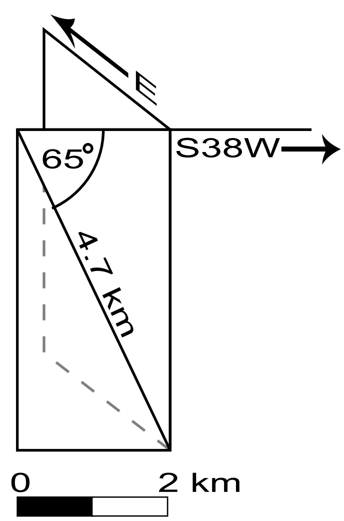

Figure 18

position, rather than absolute position, to be evaluated. In each model the established piercing line intersects the basin-bounding fault in two places creating piercing points that are separated in three dimensions on the fault surface. The line connecting these piercing points defines a three dimensional vector which is use to evaluate the net slip magnitude, net slip direction, dip-slip displacement, strike-slip displacement, and magnitude of horizontal extension.

The strain model for the Muktinath Fault is represented in figure 18a with figure 18b representing the slip vector. The block diagram is oriented parallel to the strike of the Muktinath Fault (018^{o}) at this location (fig. 18a). Connecting the formerly adjacent piercing points from either side of the Muktinath Fault produces a slip vector of magnitude 4.7 kilometers, plunging 65^{o} in the direction 218^{o} (fig. 18b). The piercing points have been displaced with a left-lateral oblique sense by 4.2 kilometers in the dip-slip direction, 1.9 kilometers in the strike-slip direction, and have undergone 0.8 kilometers of horizontal extension (fig. 18a).

The strain model for the Dangardzang Fault is representing in figure 19a with figure 19b representing the slip vector. The block diagram is oriented parallel to the strike of the Dangardzang Fault (018^{o}) at this location (fig. 19a). Connecting the formerly adjacent piercing points from either side of the Dangardzang Fault produces a slip vector of magnitude 7.1 kilometers, plunging 39^{o} in the direction 185^{o} (fig. 19b). The piercing points have been displaced with a right-lateral oblique sense by 4.5 kilometers in the dip-slip direction, 5.3 kilometers in the strike-slip direction, and have undergone 1.4 kilometers of horizontal extension (fig. 19a).

Figure 19
Model for reconstructing piercing points along the Dangardzang Fault. A - block diagram showing geometrical relationship with the offset Kagbeni Fault along the Dangardzang Fault. Gray plane represents the Dangardzang Fault which dips 74°E and 71°E. The position of the Kagbeni Fault in the hanging wall of the Dangardzang Fault is represented in red. The position of the Kagbeni Fault in the footwall of the Muktinath Fault is represented in dark blue. Light blue represents the position of the piercing line defined by the intersection of the *Bagung-Jomsom* contact with the Kagbeni Fault. The red and dark blue circles represent the piercing point defined by the intersection of this piercing line with the Dangardzang Fault surface. The red circle represents the hanging wall piercing point and the dark blue circle represents the footwall piercing point. The positions of these piercing points are projected onto axes representing increments of dip-slip, strike-slip, and extension. The magnitude of dip-slip is 4.5 km, strike-slip is 5.3 km, and extension 1.4 km. B - diagram representing the plane containing the slip vector with respect to north. The slip vector plunges 39°, trends S5° W, and has a magnitude of 7.1 km.

A. Dangardzang Fault

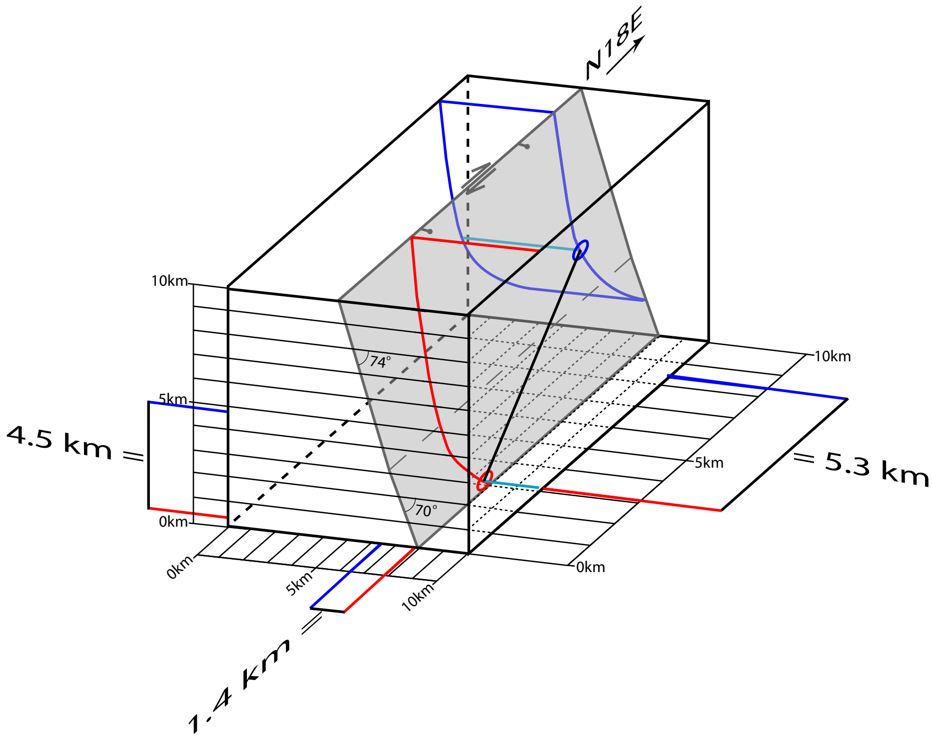

B. Dangardzang Fault
Slip Vector

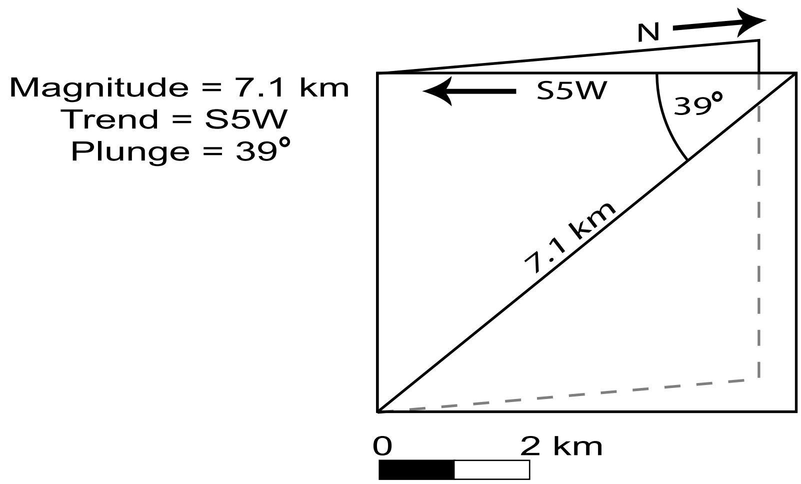

Figure 19

Discussion

Crustal-scale folding defines the deformation of the middle crust (Greater Himalayan crystallines) and upper crust (Tethyan Sedimentary sequence) during the Eocene-Oligocene (references in Kellet and Godin, 2009). In the Miocene the Annapurna-Dhaulagiri region of the Himalaya experienced oscillation between processes that have accumulated and dissipated vertical stress (fig. 20). Oligocene-Miocene crustal thickening combined with activity on the Main Central thrust in the early Miocene weakened the middle crust and elevated the Himalayan hinterland (Vannay and Hodges, 1996). This increased the vertical stress and produced a rheological contrast between the upper and middle crust that resulted in their decoupling along the Annapurna Detachment around 22-17 Ma (Kellet and Godin, 2009). This marks the first alternation between accumulation and dissipation of vertical stress for the Annapurna-Dhaulagiri region (fig. 20). Cooling of the middle crust facilitated coupling of the upper and middle crust as evidenced by the development of the Dolpo-Mugu-Manang synclinorium (Fuchs, 1964; Searle and Godin, 2003; Kellet and Godin, 2009) which deforms the hanging wall and footwall of the Annapurna Detachment (Godin et al., 2006). The formation of the Dolpo-Mugu-Manang synclinorium elevated the hinterland rocks resulting in an increase in vertical stress. Faulting within the Thakkhola Graben cross-cuts the synclinorium, effectively ending its growth as early as 14 Ma (Coleman and Hodges, 1995) and definitively by 11 Ma (Garzione et al., 2000). This marks the second alternation from accumulation to dissipation of vertical stress in this region (fig. 20). Our work shows the faults bounding the Thakkhola Graben cut the Annapurna Detachment (fig. 10a) ruling out the possibility of differential movement between the upper and lower crust after 14-

Figure 20

Time-deformation plot for the structures surrounding the Thakkhola Graben. The coupling/decoupling of the upper and middle crust as well as whether accumulation or dissipation of vertical stress is accommodated by each structure is described at the top of the plot. Main Central Thrust - operates during 22 - 13 Ma accommodating an accumulation of vertical stress in a period when the upper and lower crust are decoupled. Annapurna Detachment - operates during 22 - 17 Ma accommodating a dissipation of vertical stress in a period when the upper and lower crust are decoupled. Dolpo-Mugu-Manang Synclinorium operates during 17 - 14 Ma accommodating an increase in vertical stress during a period when the upper and lower crust are coupled. Lopukangri Rift operates during 14 - 2 Ma accommodating a dissipation in vertical stress in a period when the upper and lower crust are coupled. The Thakkhola Graben operates during 14 - present accommodating a dissipation in vertical stress during a period when the upper and lower crust are coupled. Fuchs, 1964; Coleman and Hodges, 1995; Vannay and Hodges, 1996; Garzione et al., 2000; Searle and Godin, 2003; Godin, 2006; Kellet and Godin, 2009; Murphy et al., 2010.

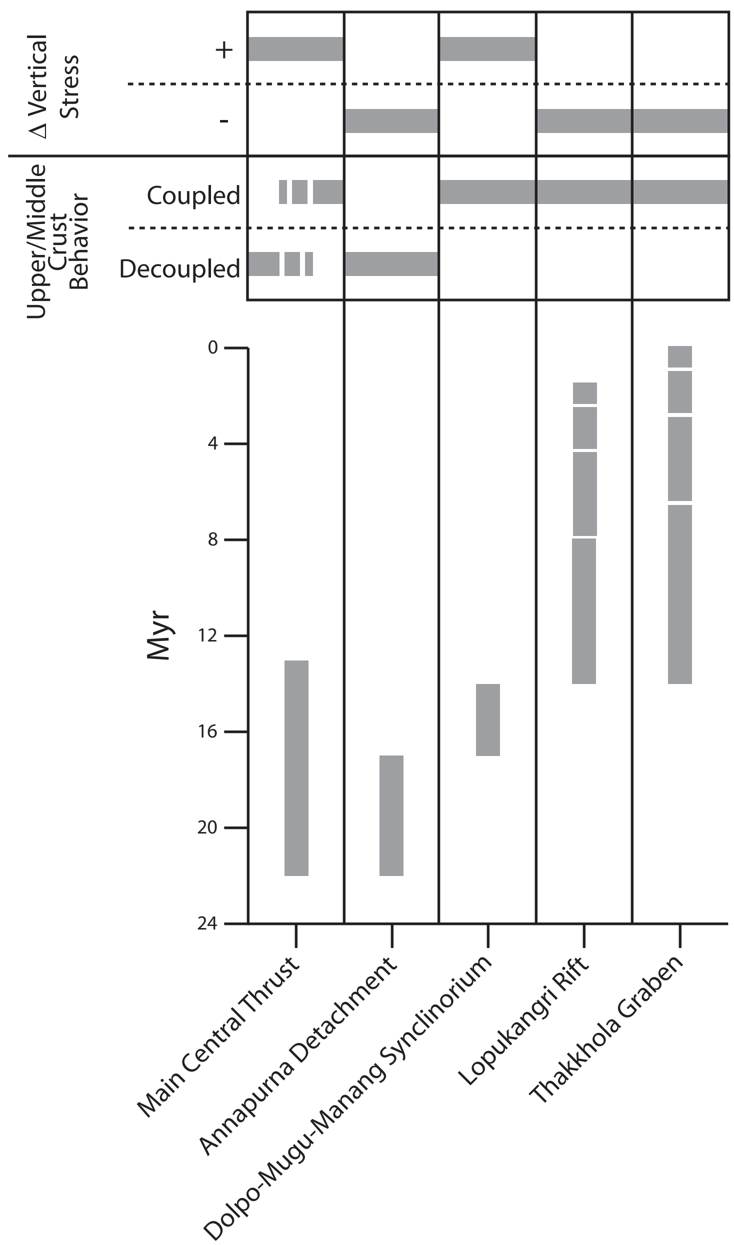

Δ Vertical Stress
+
-
Upper/Middle Crust Behavior
Coupled
Decoupled
Myr
0
4
8
12
16
20
24
Main Central Thrust
Annapurna Detachment
Dolpo-Mugu-Manang Synclinorium
Lopukangri Rift
Thakkhola Graben

Figure 20

11 Ma. Radiocarbon data provides evidence of activity as recent as 17.2 Ka on the Dangardzang Fault (Hurtado et al., 2001). The continuous operation of the Dangardzang Fault implies that the upper and middle crust have been well coupled since the middle Miocene.

Cyclic alternation between accumulation and dissipation of vertical stress has been discussed for the Annapurna and Everest regions of Nepal (Larson et al., 2010). It has been interpreted that this out-of-sequence deformation is in response to critical wedge dynamics that drive deformation towards the foreland at the Main Boundary Thrust and Main Frontal Thrust. Accumulation of vertical stress through crustal thickening in the hinterland and dissipation of that stress through foreland propagating thrust faults are linked in a process observed throughout the orogen (Larson et al., 2010). The relief of vertical stress is also accommodated within the Himalayan hinterland. This work shows that a portion of this vertical stress is being accommodated in a direction parallel to the Himalayan arc through extension along north-south oriented normal faults and graben. the Thakkhola Graben is bounded by oblique faults that accommodate convergent stress as well as vertical stress. Strike-slip motion on the Dangardzang and Muktinath Faults accommodate stress driven by N-S convergence; dip-slip motion accommodates stress driven by excess gravitational potential developed during crustal thickening.

A correlation between the Thakkhola Graben and the Lopukangri Rift (Murphy et al., 2010) can be formed on the basis of geographic position, style of faulting, and kinematic compatibility (fig. 20). Though separated by a distance of approximately 60 kilometers in an east-west direction, the Dangardzang Fault overlaps with the Lopukangri Rift for a distance of approximately 10-15 kilometers around latitude 29^{o} 45’ N. Both of

Figure 21
Map showing interaction of the Lopukangri Rift and the Thakkhola Graben at the India-Asia Suture Zone. The India-Asia Suture Zone is cut and offset by the Lopukangri Rift, geometrically suggesting the suture zone is no longer a structural boundary between India and Asia (Murphy et al., 2010). The similarity in position, timing, structural timing, and kinematics between the Lopukangri Rift and the Thakkhola Graben further imply a strong mechanical coupling across the suture zone. The Lopukangri Rift and the Thakkhola Graben potentially overlap for 10's of kilometers suggesting a structural linkage between the two. Both of these structures accommodate extension in a direction parallel to the trend of the Himalayan arc, 6.6 km at the Lopukangri Rift and 2.2 km at the Thakkhola Graben. The magnitude of net slip is approximately 10 to 12 km across both structures. This evidence implies in this region India and Asia are no longerdecoupled along the suture and have been this way since approximately 14 Ma. Murphy et al., 2010 and this work.

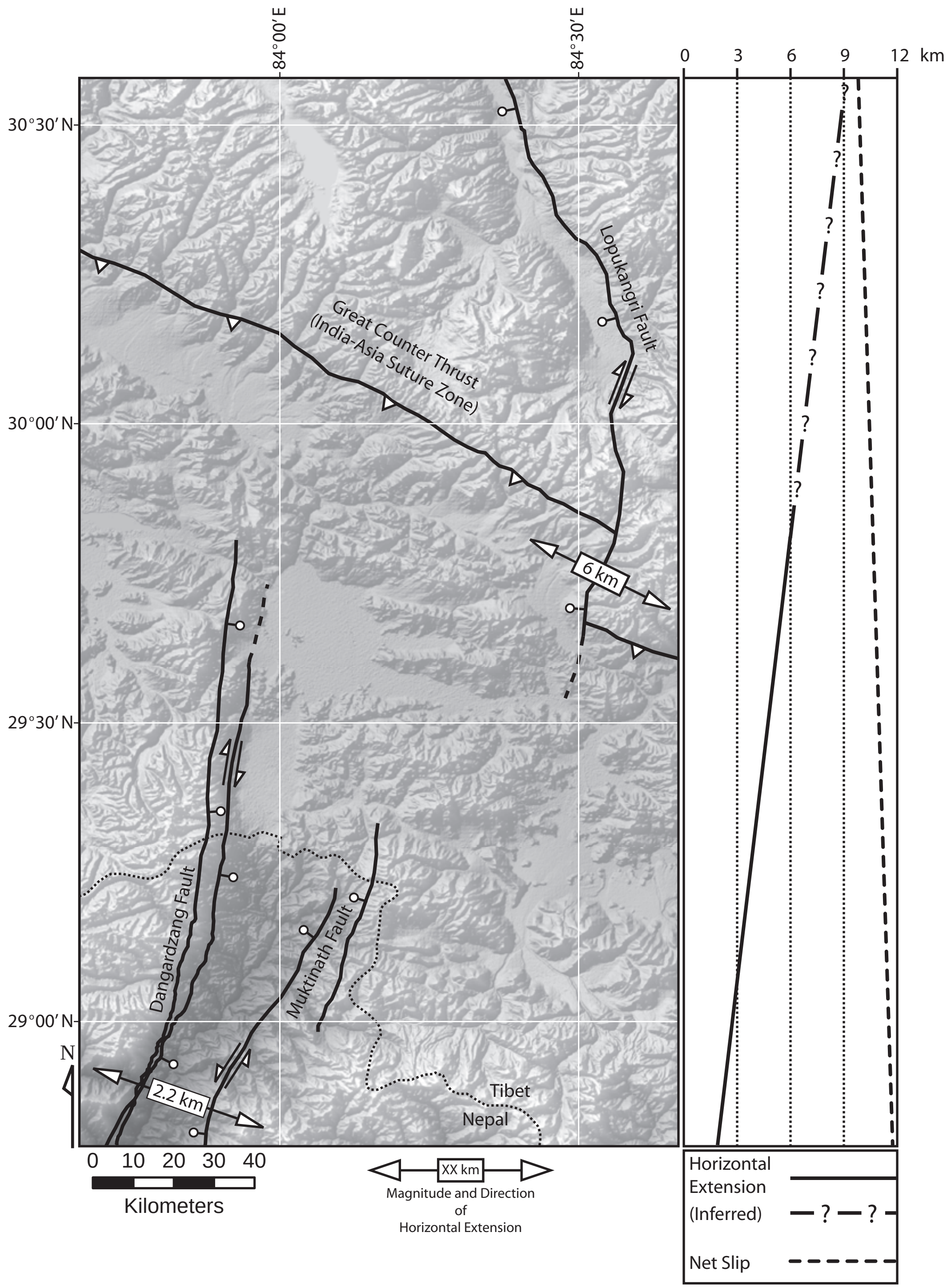

84°00′E
84°30′E
30°30′N
30°00′N
29°30′N
29°00′N
Lopukangri Fault
Great Counter Thrust
(India-Asia Suture Zone)
6 km
Dangardzang Fault
Muktinath Fault
2.2 km
Tibet
Nepal
N
0 10 20 30 40
Kilometers
XX km
Magnitude and Direction of Horizontal Extension
0 3 6 9 12 km
Horizontal Extension
(Inferred)
Net Slip

Figure 21

these structures are reported to accommodate arc-parallel extension through dip-slip displacement as well as arc-normal stress through strike-slip displacement; Lopukangri right-lateral, Muktinath left-lateral, Dangardzang right-lateral (fig. 20) (Murphy et al., 2010; this work). Net slip remains nearly constant across both of these structures at approximately 10 kilometers. The magnitude of arc-parallel extension varies from north to south with approximately 6 kilometers at Lopukangri and approximately 2.2 kilometers for the Thakkhola Graben (fig. 20). These compatibilities suggest a mechanical link between the Thakkhola Graben and the Lopukangri Rift. Lopukangri cuts and offsets the India-Asia Suture, suggesting there is no longer a mechanical boundary between Indian and Asian rocks (Murphy et al., 2010). Our results further enhance this statement by proposing that rocks on either side of the India-Asia Suture are now deforming in similar fashion and responding with the same kinematics, reinforcing the idea that India and Asia are strongly coupled in this region and have been since the middle Miocene (fig. 20).

Conclusion

Field work combined with forward modeling and geometric reconstruction of the faults bounding the Thakkhola Graben have enabled a better understanding of the geometry and kinematics of the graben as well as its relationship to surrounding structures. The faults that bound the graben cut and offset the pre-existing folded architecture of the Tethyan Sedimentary sequence. Our mapping reveals the presence of the Kagbeni Fault, a steeply north-dipping reverse fault that runs across the field area and is offset by the graben-bounding faults. A structural and metamorphic discontinuity termed the Mustang Detachment is observed near the Nepal-Tibet border and we propose this may be the expression of the brittle upper detachment of the South Tibetan Detachment System. The western boundary of the Thakkhola Graben is the Dangardzang Fault which consists of two steeply dipping, parallel fault strands; the easternmost of which shallows at depth from 74^{o}E to 67^{o}E. Slip along the Dangardzang Fault is oblique with a 4.5 kilometer normal dip-slip component and a 5.3 kilometer dextral strike-slip component. Strike-slip motion is recorded for the eastern Dangardzang Fault and no evidence of strike-slip is observed on the western Dangardzang Fault. The magnitude of horizontal extension accommodated by the Dangardzang Fault is 1.4 kilometers. The eastern boundary of the Thakkhola Graben is the Muktinath Fault which consists of one dominant fault strand that dips 81^{o}W and several subsidiary faults of varying magnitudes. Slip along the Muktinath Fault is oblique with a 4.2 kilometer normal dip-slip component and a 1.9 kilometer sinistral strike-slip component. Fault striae on the Dangardzang and Muktinath Faults suggest an early phase of strike-slip dominated oblique-slip followed by a later phase of almost pure dip-slip. The basin-fill formations have been folded into graben-parallel kink folds with homoclinal dip panels. These folds are interpreted to have formed via inclined shear imparted to the hanging wall while passing over bends in the Dangardzang Fault surface during increments of slip. Field mapping combined with ASTER and Google Earth satellite imagery highlight the relationship of the Dolpo-Mugu leaucogranite to the Mustang leaucogranite. These have been previously described as two separate bodies, but our work reveals no obvious boundary between the two. This suggests they are the same body or requires the presence of an undetected intervening structure. The region surrounding the Thakkhola Graben has experienced compressive deformation in response to stress from the collision of India with Asia as well as extensional deformation in response to elevation of topography beyond a stable threshold. This combined with a dynamic history of coupling and decoupling of the upper and middle crustal rocks has resulted in a superposition of a variety of structures. Through normal faulting the Thakkhola Graben accommodates a dissipation of vertical stress that was accumulated during the growth of the Dolpo-Mugu-Manang synclinorium; concurrent strike-slip faulting along the bounding faults has accommodated convergent stress imposed by basal shear during convergence. The faults bounding the Thakkhola Graben cut steeply through the upper and middle crust necessitating strong mechanical coupling between these two layers. The proximity and kinematic similarity between the Thakkhola Graben and the Lopukangri Rift suggest a cogenetic and mechanical relationship between the two. This relationship implies there is no longer a structural and mechanical discontinuity across the suture between India and Asia, rather these two continental blocks are strongly coupled and deform under the same stress field in the central part of the orogen.

References

Armijo, R., P. Tapponnier, H. Tonglin (1989), Late Cenozoic right-lateral strike-slip faulting in southern Tibet, *Journal of Geophysical Research*, v. 94, no. B3, 2,787-2,838.

Baltz, T.K., M.A. Murphy (2009), Structural evolution of the Thakkhola Graben and implications on the architecture of the central Himalaya, Fall AGU Meeting, San Francisco.

Bassoullet, J.P., M. Colchen (1974), Les formations tardi-orogeniques de la Thakkhola, Himalaya du Nepal. *2nd Reun. Sci. Terre, Soc. Geol.*, France, 34.

Bodenhausen, J.W.A., T. De Booy, C.G. Egeler, H.J. Nijhuis (1964) On the Geology of Central-West Nepal - A Preliminary Note, Rep. 22nd International Geologic Congress, Delhi, XI, 101–122.

Bordet, P., M. Colchen, D. Krummenacher, P. Le Fort, R. Mouterde, J.M. Reme (1967), Esquisse Geologiques de la Thakkhola (Nepal Central), Paris, C.N.R.S., scale 1:75,000.

Bordet, P., M. Colchen, D. Krummenacher, P. Le Fort, R. Mouterde, J.M. Reme (1971), *Recherches Geologiques dans l'Himalaya du Nepal: Region de la Thakkhola*, Paris, C.N.R.S., 279 p.

Bordet, P., M. Colchen, P. Le Fort (1975), *Recherchers Geologiques dans l'Himalaya du Nepal, Region du Nyi-Shang*, Paris, C.N.R.S., 138 p.

Brown, R.L., J.H. Nazarchuk (1993), Annapurna detachment fault in the Greater Himalaya of central Nepal, in *Himalayan Tectonics*, eds. P.J. Treloar, M.P. Searle, *Geological Society of London Special Publication 74*, 461-473.

Burbank, D.W., R.A. Beck, T. Mulder (1996), The Himalayan foreland basin, in *The Tectonics of Asia,* eds. A. Yin, T.M. Harrison, 149–88, New York, Cambridge University Press.

Burchfiel, B.C., L.H. Royden (1985), North-south extension within the convergent Himalayan region, *Geology*, v. 13, 679-682.

Burchfiel, B.C., Z. Chen, K.V. Hodges, Y. Liu, L.H. Royden, C. Deng, J. Xu (1992), *The South Tibetan detachment system, Himalayan orogen: Extension contemporaneous with and parallel to shortening in a collisional mountain belt*, *Geological Society of America Special Paper* 269, Boulder, Colorado, 41 p.

Chen Q., J.T. Freymueller, Z. Yang, C. Xu, W. Jiang, Q. Wang, J. Liu (2004), Spatially variable extension in southern Tibet based on GPS measurements, *Journal of Geophysical Research*, v. 109, doi: 10.1029/2002JB002350.

Colchen, M., P. Le Fort, A. Pecher (1981), Geological Map of Annapurna-Manaslu-Ganesh Himalaya, Nepal, in *Zagros-Hindu Kush-Himalaya Geodynamic Evolution*, eds. Gupta, H.K. and Delaney, F.M., eds., Washington, D.C., American Geophysical Union, scale 1:200,000.

Colchen, M., M. Fort, P. Freytet (1980) Evolution paleogeographique et structural du fosse de la Thakkhola-Mustang (Himalaya du Nepal) implications sur l'evolution recente de la chanie Himalayanne, *C.R. Acad. Sci. Paris*, 280, 311-314.

Colchen, M., P. Le Fort, A. Pecher (1986), *Recherches Geologiques dans l'Himalaya du Nepal: Annapurna-Manaslu-Ganesh Himal*, Paris, C.N.R.S., 136 p.

Colchen, M. (1999), The Thakkhola-Mustang Graben in Nepal and the Late Cenozoic extension in the Higher Himalayas, *Journal of Asian Earth Sciences*, v. 17, 683-702.

Coleman, M., K.V. Hodges (1995), Evidence for Tibetan Plateau uplift before 14 Myr ago from a new minimum age for east-west extension, *Nature*, v. 374, 49-50.

Copley, A. and D. McKenzie (2007), Models of crustal flow in the India-Asia collision zone, *Geophysical Journal International*, v. 169, 683-698.

Debon, F., P. Le Fort, S.M.F. Sheppard, J. Sonet (1986), The four plutonic belts of the Transhimalaya-Himalaya: A chemical, mineralogical, isotopic, and chronological synthesis along a Tibet-Nepal section, *Journal of Petrology*, v. 27, 281-302.

Edwards, M.A., T.M. Harrison (1997), When did the roof collapse? Late Miocene N-S extension in the High Himalaya revealed by Th-Pb monazite dating of the Khula Kangri Granite, *Geology*, v. 25, 543-546.

Fort, M., P. Freytet, M. Colchen (1982), Structural and sedimentological evolution of the Thakkhola Mustang graben (Nepal Himalaya), *Z. fur Geomorph. Suppl. Bd*, 42, 75-98.

Fuchs, G. (1964), Note on the geology of the Paleozoics and Mesozoics of the Tibetan Zone of the Dolpo region (Nepal-Himalaya), *Verhandl Geol. Bundesandt*., 6-15.

Fuchs, G. (1967), Zum Bau des Himalaya, Denkschr. Osterr. Akad. Wiss., math.-naturw. v. 113, 1-211.

Fuchs, G. (1977), The geology of the Karnali and Dolpo regions, Western Nepal, *Jahrb. Geol. Bundesandt*., Austria, v. 120, 165-217.

Fuchs, G., R.W. Ridder, R. Tuladhar (1988), Contributions to the geology of the Annapurna Range (Manang area, Nepal), *Jahrb. Geol. Bundesandt,* Austria, v. 131, 593-607.

Gansser, A. (1964), *Geology of the Himalayas*, Wiley, New York, 289 p.

Garzanti, F., M.P. Frette (1991), Stratigraphic succession of the Thakkhola region (Central Nepal) – Comparison with the northwestern Tethys Himalaya, *Riv. It. Paleont. Strat.*, v. 97, no. 1, 3-26.

Garzanti, E. (1999), Stratigraphy and sedimentary history of the Nepal Tethys Himalaya passive margin, *Journal of Asian Earth Sciences*, v. 17, 805-827.

Garzione, C.N., D.L. Dettman, J. Quade, P.G. DeCelles, R.F. Butler (2000), High times on the Tibetan Plateau: Paleoelevation of the Thakkhola Graben, Nepal, *Geology*, v. 28, 339–342.

Garzione, C.N., P.G. Decelles, D.G. Hodkinson, T.P. Ojha, B.N. Upreti (2003), East-west extension and Miocene environmental change in the southern Tibetan Plateau: Thakkhola Graben, Central Nepal, *Geological Society of America Bulletin*, v. 115, no. 1, 3-20.

Gradstein, F.M., M.R. Gibling, M. Sarti, U. Von Rad, J.W. Thurow, J.G. Ogg, L.F. Jansa, M.A. Kaminski, G.E.G. Westermann (1991), Mesozoic Tethyan strata of Thakkhola, Nepal: Evidence for the drift and breakup of Gondwana, *Palaeogeogr., Palaeoclimatol., Palaeoecol.,* v. 88, 192-218.

Godin, L., R.L. Brown, S. Hanmer, R. Parrish (1999a), Back folds in the core of the Himalayan orogen: An alternative interpretation, *Geology*, v. 27, no. 2, 151-154.

Godin, L., R.L. Brown, S. Hanmer (1999b), High Strain Zone in the Hanging Wall of the Annapurna Detachment, Central Nepal Himalaya, in *Himalaya and Tibet: Mountain Roots to Mountain Tops*, eds. A. Macfarlane, R.B. Sorkhabi, J. Quade, *Geological Society of America Special Paper 328*, Boulder, Colorado, 199-210.

Godin, L., R.R. Parrish, R.L. Brown, K.V. Hodges (2001), Crustal thickening leading to exhumation of the Himalayan metamorphic core of Central Nepal: Insight from U-Pb geochronology and $^{40}Ar/^{39}Ar$ thermochronology, *Tectonics*, v. 20, no. 5, 729-747.

Godin, L. (2003), Structural evolution of the Tethyan sedimentary sequence in the Annapurna area, central Nepal Himalaya, *Journal of Asian Earth Sciences*, v. 22, 307-328.

Hagen, T. (1959), Geologie des Thakkhola (Nepal), *Eclogae Geologicae Helveticae*, v. 52, 709-720.

Harrison, T.M., P. Copeland, W.S.F. Kidd, O. Lovera (1995), Activation of the Nyainquentanghla Shear Zone: Implications for uplift of the southern Tibetan Plateau, *Tectonics*, v. 14, 658–676.

Harrison, T.M., F.J. Ryerson, P. Le Fort, A. Yin, O.M. Lovera, E.J. Catlos (1997), A Late Miocene-Pliocene origin for the Central Himalayan inverted metamorphism, *Earth Planet. Sci. Lett.*, v. 146, 1-8.

Harrison, T.M., M. Grove, K.D. McKeegan, C.D. Coath, O.M. Lovera, P. Le Fort (1999), Origin and episodic emplacement of the Manaslu Intrusive Complex, *Journal of Petrology*, v. 40, no. 1, 3-19.

Hodges, K.V., R.R. Parrish, M.P. Searle (1996), Tectonic evolution of the central Annapurna Range, Nepalese Himalayas, *Tectonics*, v. 15, 1264–1291.

Hurtado, J.M., K.V. Hodges, K.X. Whipple (2001), Neotectonics of the Thakkhola graben and implications for recent activity on the South Tibetan fault system in the central Nepal Himalaya, *Geological Society of America Bulletin*, v. 13, 222-240.

Jade, S., B. Bhatt, Z. Yang, R. Bendick, V. Gaur, P. Molnar, M. Anand, D. Kumar (2004), GPS measurements from the Ladakh Himalaya, India: Preliminary tests of plate-like or continuous deformation in Tibet, *Geological Society of America Bulletin*, v. 116, 1385.

Jessup, M.J., D.L. Newell, J.M. Cottle, A.L. Berger, J.A. Spotila (2008) Orogen-parallel extension and exhumation enhanced by focused denudation in the Arun River Gorge, Ama Drime Massif, Tibet-Nepal, *Geology*, v. 36, 587-590.

Kali, E., P.H. Leloup, N. Arnaud, G. Maheo, D. Liu, E. Boutonnet, J. Van Der Woerd, X. Liu, J. Liu-Zeng, H. Li (2010), Exhumation history of the deepest central Himalayan rocks, Ama Drime Range: Key pressure-temperature-deformation-time constraints on orogenic models, *Tectonics*, v. 29, no. 2, doi: 10.1029/2009TC002551.

Klootwijk, C.T., F.S. Gee, J.W. Peirce, G.M. Smith, P.L. McFadden (1992), An early India contact: Paleomagnetic constraints from Ninetyeast Ridge, ODP Leg 121, *Geology*, v. 20, 395-398.

Le Fort, P. (1975), Himalayas: The collided range. Present knowledge of the continental arc, *American Journal of Science*, v. 275-A, 1-44.

Le Fort, P., C. France-Lanord (1995), Granites from Mustang and surrounding regions (Central Nepal), *Journal of Nepal Geological Society,* v. 11, 53-57.

Leloup, P.H., G. Maheo, N. Arnoud, E. Kali, E. Boutonnet, D. Liu, L. Xiaohan, L. Haibing (2010), The South Tibet Detachment Shear Zone in the Dinggye area time constraints on extrusion models of the Himalayas, *Earth and Planetary Science Letters,* v. 292, 1-16.

Lee, J., C. Hager, S.R. Wallis, D.F. Stockli, M.J. Whitehouse, M. Aoya, Y. Wang (2011), Middle to late Miocene extremely rapid exhumation and thermal reequilibration in the Kung Co Rift, Southern Tibet, *Tectonics,* doi:10.1029/2010TC002745.

McCaffrey, R. and J. Nabelek (1998), Role of oblique convergence in the active deformation of the Himalayas and Southern Tibetan Plateau, *Geology*, v. 26, 691-694.

Molnar, P., P. Tapponnier (1978), Active tectonics of Tibet, *Journal of Geophysical Research*, v. 83, no. B11, 5,361-5,375.

Molnar, P. (1984), Structure and tectonics of the Himalaya: Constraints and implications of geophysical data, *Annu. Rev. Earth Planet. Sci.,* v. 12, 489-518.

Murphy, M.A., T.M. Harrison (1999), The relationship between leucogranites and the South Tibetan Detachment System, Rongbuk Valley, Southern Tibet, *Geology*, v. 27, 831-834.

Murphy, M.A., A. Yin, P. Kapp, T.M. Harrison, D. Lin, G. Jinghui (2000) Southward propagation of the Karakoram Fault System, Southwest Tibet: Timing and magnitude of slip, *Geology*, v. 28, 451-454.

Murphy, M.A., A. Yin, P. Kapp, T. Harrison, C, Manning, F. Ryerson, D. Lin, G. Jinghui (2002), Structural evolution of the Gurla Mandhata Detachment System, Southwest Tibet: Implications for the eastward extent of the Karakoram Fault System, *Geological Society of America Bulletin*, v. 114, 428-447.

Murphy, M.A. and P. Copeland (2005), Transtensional deformation in the central Himalaya and its role in accommodating growth of the Himalayan orogen, *Tectonics*, v. 24, doi: 10.1029/2004TC001659.

Murphy, M.A., V. Sanchez, M.H. Taylor (2010), Syncollisional extension along the India-Asia Suture Zone, South-Central Tibet: Implications for crustal deformation of Tibet, *Earth and Planetary Science Letters*, v. 290, 233-243.

Nakata, T., K. Otsuki, S.H. Khan (1990), Active faults, stress field, and plate motion, along the Indo-Eurasian Plate boundary, *Tectonophysics*, v. 181, 83-95.

Noble, S.R. and M.P. Searle (1995), Age of crustal melting and leucogranite formation from U-Pb zircon and monazite dating in the Western Himalaya, Zanskar, India, *Geology*, v. 23, 1135-1138.

Pecher, A. (1978), *Deformations et metamorphisme associes a une zone de cisaillement: Exemple du Grand Chevauchement Central Himalayan (MCT)*, D. Sc. Thesis, Univ. Grenoble, France, 354 p.

Peltzer, G., P. Tapponnier (1988), Formation and evolution of strike-slip faults, rifts, and basins during the India-Asia collision, An experimental approach, *Journal of Geophysical Research*, v. 93, no. B12, 15,085-15,117.

Ratschbacher, L., W. Frisch, G. Lui, C. Chen (1994), Distributed deformation in southern and western Tibet during and after the India-Asia collision, *Journal of Geophysical. Research*, v. 99, 19,817-19,945.

Replumaz, A., P. Tapponnier (2003), Reconstruction of the deformed collision zone between India and Asia by backward motion of lithospheric blocks, *Journal of Geophysical Research*, v. 108, no. B6, doi: 10.1029/2001JB000661.

Searle, M.P., L. Godin (2003), The South Tibetan detachment and the Manaslu leucogranite: A structural reinterpretation and restoration of the Annapurna-Manaslu Himalaya, Nepal, *The Journal of Geology*, v. 111, p. 505-523.

Seeber, L. and A. Pêcher (1998), Strain partitioning along the Himalayan arc and the Nanga Parbat antiform, *Geology*, v. 26, 791-794.

Scharer, U., R. Xu, C. J. Allegre (1986), U-(Th)-Pb systematics and ages of Himalayan leucogranites, South Tibet, *Earth and Planetary Science Letters*, v. 77, 35-48.

Schill, E., E. Appel, C. Crouzet, P. Gautam, F. Wehland, M. Staiger (2004), Oroclinal bending versus regional significant clockwise rotations in the Himalayan arc – Constraints from secondary pyrrhotite remanences, in *Orogenic Curvature: Integrating Paleomagnetic and Structural Analyses*, eds. A.J. Sussman, A.B. Weil, *Geological Society of America Special Papers 383*, 73-85.

Styron, R.H., M.H. Taylor, M.A. Murphy (2009), Himalayan orogen-parallel extension from GPS geodesy and structural geology, 5th International Symposium on Tibetan Plateau-24th Himalaya-Karakoram-Tibet-Workshop, Beijing, China, 11-14.

Styron, R.H., M.H. Taylor, M.A. Murphy (2011), Oblique convergence, arc-parallel extension, and the role of strike-slip faulting in the High Himalaya, *Geosphere*, v. 7, 1-15.

Tapponnier P., G. Peltzer, A. Y. Le Dain, R. Armijo, P. Cobbold (1982), Propagating extrusion tectonics in Asia: New insights from simple experiments with plasticine, *Geology*, v. 10, 611-616.

Thiede, R.C., J.R. Arrowsmith, B. Bookhagen, M. McWilliams, E.R. Sobel, M.R. Strecker (2006), Dome formation and extension in the Tethyan Himalaya, Leo Pargil, Northwest India, *Geological Society of America Bulletin*, v. 118, no. 5-6, 635-650.

Wu, C., K.D. Nelson, G. Wortman, S. Samson, Y. Yue (1998), Yadong cross structure and South Tibetan Detachment in the East Central Himalaya (898–908E), *Tectonics*, v. 17, 28-45.

Xiao, H., J. Suppe (1992), Origin of rollover, *AAPG Bulletin*, v. 76, 509-529.

Yin, A. and T.M. Harrison (2000), Geologic evolution of the Himalayan-Tibetan orogen, *Annual Review of Earth and Planetary Sciences*, v. 28, 211-280.

Zhang, H., N. Harris, R.R. Parrish, S. Kelley, L. Zhang, N. Rogers, T. Argles, J. King (2004), Causes and consequences of protracted melting of the mid-crust exposed in the North Himalayan antiform, *Earth and Planetary Science Letters*, v. 228, 195-212.

Zhao, W. and K.D. Nelson (1993), Project INDEPTH 1993, Deep seismic reflection evidence for continental underthrusting beneath southern Tibet, *Nature*, 366, 557-559.